

PAPER • OPEN ACCESS

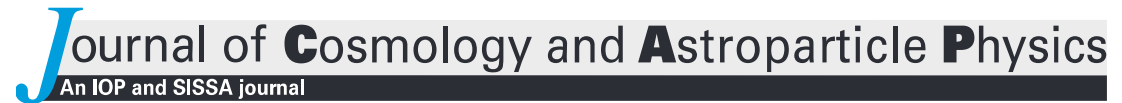
A cosmological sandwiched window for leptonnumber breaking scale

To cite this article: Shao-Ping Li and Bingrong Yu JCAP04(2024)047

View the <u>article online</u> for updates and enhancements.

You may also like

- Supernova constraints on massive (pseudo)scalar coupling to neutrinos Lucien Heurtier and Yongchao Zhang
- Cold light dark matter in extended seesaw models
 Sami Boulebnane, Julian Heeck, Anne Nguyen et al.
- Probing beyond the standard model physics with double-beta decays Elisabetta Bossio and Matteo Agostini



RECEIVED: October 29, 2023 REVISED: February 13, 2024 ACCEPTED: March 4, 2024 PUBLISHED: April 16, 2024

A cosmological sandwiched window for lepton-number breaking scale

Shao-Ping Li \mathbb{D}^a and Bingrong Yu $\mathbb{D}^{a,b}$

^aInstitute of High Energy Physics, Chinese Academy of Sciences, Beijing 100049, China

^bDepartment of Physics, LEPP, Cornell University, Ithaca, NY 14853, U.S.A.

E-mail: spli@ihep.ac.cn, bingrong.yu@cornell.edu

ABSTRACT: A singlet majoron can arise from the seesaw framework as a pseudo-Goldstone boson when the heavy Majorana neutrinos acquire masses via the spontaneous breaking of global $U(1)_L$ symmetry. The resulting cosmological impacts are usually derived from the effective majoron-neutrino interaction, and the majoron abundance is accumulated through the freeze-in neutrino coalescence. However, a primordial majoron abundance can be predicted in a minimal setup and lead to distinctive cosmological effects. In this work, we consider such a primordial majoron abundance from relativistic freeze-out and calculate the modification to the effective neutrino number $N_{\rm eff}$. We demonstrate that the measurements of $N_{\rm eff}$ will constrain the parameter space from a primordial majoron abundance in an opposite direction to that from neutrino coalescence. When the contributions from both the primordial abundance and the freeze-in production coexist, the $U(1)_L$ -breaking scale (seesaw scale) f will be pushed into a "sandwiched window". Remarkably, for majoron masses below 1 MeV and above the eV scale, the future CMB-S4 experiment will completely close such a low-scale seesaw window for $f \in [1, 10^5]$ GeV. We highlight that any new light particle with a primordial abundance that couples to Standard Model particles may lead to a similar sandwiched window, and such a general phenomenon deserves careful investigation.

KEYWORDS: cosmological neutrinos, cosmology of theories beyond the SM, particle physics - cosmology connection, physics of the early universe

ARXIV EPRINT: 2310.13492

\mathbf{C}	ontents				
1					
2					
	2.1 The singlet majoron model	3			
	2.2 Majoron cosmology in the low-scale seesaw scenario	5			
3	Analytical derivation of $\Delta N_{ m eff}$ from majoron decay	7			
	3.1 Relativistic freeze-out and relativistic decay	8			
	3.2 Relativistic freeze-out and nonrelativistic decay	10			
	3.3 Freeze-in without primordial majoron	10			
	3.4 Comparison between freeze-out and freeze-in	12			
4	Calculation of $\Delta N_{ m eff}$ beyond instantaneous majoron decay	13			
5	The sandwiched window from precision $N_{ m eff}$ measurements	17			
6	Conclusions	20			
A	Majoron interactions	21			
	A.1 Majoron-neutrino interactions	21			
	A.2 Majoron-Higgs interactions	24			
В	Neutrino coalescence rate	26			

1 Introduction

Over the past few decades, cosmological observations have reached unprecedented precision, which offers a promising avenue for probing new physics beyond the Standard Model (SM). For instance, nowadays the measurements of the effective number of neutrino species $N_{\rm eff}$ have reached the accuracy of $\mathcal{O}(0.1)$ through the observations of big bang nucleosynthesis (BBN) and cosmic microwave background (CMB) [1, 2]. In general, any new light particles coupling to the SM particles might contribute to the relativistic degrees of freedom in the early universe and lead to significant deviations from the SM prediction of $N_{\rm eff}$, and therefore will receive strict constraints from cosmology.

In this work, we revisit the majoron-neutrino interactions under the cosmological constraints of N_{eff} and study their possible implications for the low-scale seesaw scenario. A singlet majoron J can naturally arise as a pseudo-Goldstone boson [3] in the framework of the type-I seesaw model [4–8], where the heavy Majorana neutrinos acquire masses through the spontaneous breaking of the global $U(1)_L$ lepton-number symmetry. The lepton-number breaking scale f characterizes the mass scale of heavy neutrinos, i.e., the scale of new physics responsible for the origin of neutrino masses. After the electroweak gauge symmetry breaking,

the majoron will couple with the SM neutrinos ν_i through the mixing between active and sterile neutrinos, where the couplings are suppressed by m_i/f (with m_i the mass of ν_i). Therefore, the majoron is expected to be long-lived due to the large hierarchy between m_i and f, which makes the majoron an interesting candidate of dark matter (DM) [9–17]. For a relatively low breaking scale $f \lesssim 100\,\text{TeV}$, which corresponds to the low-scale seesaw scenario, the decay of the majoron into a pair of SM neutrinos could occur and contribute to N_{eff} at some crucial epochs of the Universe, leaving observable imprints in, e.g., the BBN and CMB. Given the strict constraints on N_{eff} from current and upcoming CMB experiments [1, 22–25], it is hopeful that we could probe the mechanism for neutrino mass generation from observables in the early Universe.

The constraints on the lepton-number breaking scale from $N_{\rm eff}$ have been noticed for a while [26–30], mostly in a model-independent setup. In previous works, the primordial abundance of the majoron was usually neglected such that the majoron abundance was initialized via the effective interaction between the active neutrinos and the majoron. In particular, for a light majoron below the MeV scale, the majoron abundance is accumulated through the freeze-in $2\nu \to J$ process where the majoron-neutrino coupling is sufficiently small. In this case, the primordial majoron abundance is negligible before the SM neutrino decoupling, and the decay of the majoron into a pair of neutrinos $J \to 2\nu$ after the SM neutrino decoupling will inject energies into neutrinos, causing an excess of $N_{\rm eff}$. Consequently, a smaller breaking scale f (equivalent to a larger majoron-neutrino coupling) brings about a larger majoron abundance, thereby leading to a larger deviation of $N_{\rm eff}$. Therefore, the constraints from the $N_{\rm eff}$ measurements will put a lower bound on f in the freeze-in situation.

However, a primordial majoron abundance generated beyond the effective majoronneutrino interaction in general cannot be neglected before the SM neutrino decoupling. In fact, it can be predicted even in a minimal setup and more importantly, it may have a sizable effect to $N_{\rm eff}$. In this work, we investigate such an effect that has usually been neglected in the literature. We focus on the situation where the majoron is assumed to be in thermal equilibrium with SM particles in the early Universe, such that the primordial majoron abundance is inherited from relativistic freeze-out. As can be seen later, this situation is easy to realize, either via the interactions between the majoron and the heavy Majorana neutrinos or through the majoron-Higgs interactions in the scalar sector. We will also consider the situation where the primordial majoron abundance is accumulated by some other mechanism beyond the relativistic freeze-out.

The primordial majoron abundance will lead to several interesting phenomena. First of all, for a non-negligible primordial abundance, if it exists before the SM neutrino decoupling but is only depleted into radiation near the recombination epoch, $N_{\rm eff}$ will be drastically increased by orders of magnitude (see section 3.2). Therefore, the precision measurements of $N_{\rm eff}$ at the CMB epoch will severely constrain the abundance, and put strict bounds on the ultraviolet (UV) physics that features the abundance. Furthermore, for nonrelativistic majoron decay, a larger breaking scale f leads to later decay, and hence a larger modification to $N_{\rm eff}$. So the

¹If the U(1)_L global symmetry is only broken spontaneously, then the majoron will be strictly massless as a real Nambu-Goldstone boson. However, to serve as a DM candidate, the majoron should acquire a nonzero mass where the global symmetry is broken explicitly [11, 18–21].

constraints from $N_{\rm eff}$ will put an upper bound on f, in contrast to the freeze-in situation. This is particularly interesting because when the freeze-in and primordial abundances coexist, the constraint from the $N_{\rm eff}$ measurements will push f into a sandwiched window. Remarkably, the next-generation CMB experiments could further narrow or completely close such a sandwiched window [22–25].

The remaining part of this paper is organized as follows. In section 2, we start with a brief review of the singlet majoron model. Then we perform a general analysis of the majoron evolution in the early Universe and its cosmological impacts. In section 3, we derive $N_{\rm eff}$ using an approximate analytical (but intuitive) method by assuming instantaneous majoron decay. A stricter calculation of $N_{\rm eff}$ beyond instantaneous majoron decay is conducted in section 4. The constraints on f from $N_{\rm eff}$ are given in section 5, which provide a cosmological sandwiched window for the low-scale seesaw scenario. We summarize our main results in section 6. Finally, some technical details are included in the appendices.

2 Framework

2.1 The singlet majoron model

The singlet majoron model [3] introduces a complex scalar S, which is a singlet under the SM gauge symmetries. The relevant Lagrangian in the Yukawa sector is given by

$$\mathcal{L} = -\overline{\ell_{\rm L}} Y_{\nu} \widetilde{\Phi} N_{\rm R} - \frac{1}{2} \overline{N_{\rm R}^c} Y_N N_{\rm R} S + \text{h.c.}, \qquad (2.1)$$

where $\ell_{\rm L}=(\nu_{\rm L},l_{\rm L})^{\rm T}$ and $\widetilde{\Phi}\equiv {\rm i}\sigma^2\Phi^*$ are the left-handed lepton doublet and the Higgs doublet, respectively. Y_{ν} is the Dirac neutrino Yukawa coupling matrix, and Y_N is the Yukawa coupling matrix for the right-handed (RH) neutrino singlets $N_{\rm R}$, where $N_{\rm R}^c\equiv C\overline{N_{\rm R}}^{\rm T}$ has been defined with $C={\rm i}\gamma^2\gamma^0$ the charge-conjugation matrix.

The Lagrangian in eq. (2.1) owns a global $U(1)_L$ symmetry if we assign the lepton numbers of relevant particles to be: $L(\ell_L) = L(N_R) = +1$, $L(\Phi) = 0$, and L(S) = -2. This global symmetry is spontaneously broken after S acquires a non-zero vacuum expectation value (VEV) from the scalar potential (see appendix A.2 for the discussion about a general scalar potential obeying the lepton-number conservation)

$$V \supset \mu_S^2 \left(S^{\dagger} S \right) + \frac{\lambda_S}{2} \left(S^{\dagger} S \right)^2.$$
 (2.2)

In this work, we adopt the linear realization of the broken symmetry. That is, the complex scalar is parametrized as^2

$$S = \frac{1}{\sqrt{2}} (f + \rho + iJ),$$
 (2.3)

where ρ and J are two real degrees of freedom. In addition, f is the scalar VEV, corresponding to the lepton-number breaking scale, which provides a Majorana mass term $M_{\rm R} = Y_N f/\sqrt{2}$ for the RH neutrinos. Note that f is also the seesaw scale provided $\mathcal{O}(Y_N) \simeq \mathcal{O}(1)$, i.e.,

²See ref. [11] for the nonlinear realization of the broken $U(1)_L$ symmetry, where S is parametrized as $S = (\rho + f) e^{iJ/f}/\sqrt{2}$.

 $f \simeq \mathcal{O}(M_{\rm R})$, which is usually considered as the UV completion of the canonical seesaw model [4–8].

From eq. (2.2), it is easy to show that ρ will acquire a mass proportional to f after the lepton-number breaking while J remains massless. Therefore, the pseudo-scalar J (i.e., the majoron) is identified as the Goldstone boson of the spontaneous $U(1)_L$ symmetry breaking. In practice, a non-zero majoron mass m_J can be generated by adding terms that explicitly violate the $U(1)_L$ symmetry, at either tree or loop levels [11, 18–21]. A simple case of mass generation is discussed in appendix A.2. In the following analysis, we will simply treat the majoron mass as a free parameter.

After the breaking of the electroweak gauge symmetry, the majoron can interact with active neutrinos through the flavor mixing between active and sterile neutrinos. The general interaction in the mass basis turns out to be [31]

$$\mathcal{L}_{J} = -\frac{\mathrm{i}J}{2f} \sum_{i,j=1}^{6} \overline{n_{i}} \left[\gamma_{5} \left(m_{i} + m_{j} \right) \left(\frac{1}{2} \delta_{ij} - \operatorname{Re} \mathcal{C}_{ij} \right) + \mathrm{i} \left(m_{i} - m_{j} \right) \operatorname{Im} \mathcal{C}_{ij} \right] n_{j}.$$
 (2.4)

A detailed derivation is presented in appendix A.1. In eq. (2.4), n_i denotes the neutrino mass eigenstate with mass m_i , and the indices i = 1, 2, 3 (i = 4, 5, 6) correspond to the active (sterile) neutrino species. The mixing parameters $C_{ij} \equiv \sum_{k=1}^{3} U_{ki}^* U_{kj}$ are defined by the 6×6 unitary matrix \mathcal{U} which diagonalizes the neutrino mass matrix via

$$\mathcal{U}^{\dagger} \begin{pmatrix} 0 & M_{\mathrm{D}} \\ M_{\mathrm{D}}^{\mathrm{T}} & M_{\mathrm{R}} \end{pmatrix} \mathcal{U}^{*} = \operatorname{Diag} \left(m_{1}, m_{2}, \dots, m_{6} \right), \tag{2.5}$$

with $M_{\rm D}=Y_{\nu}v/\sqrt{2}$ the Dirac neutrino mass matrix and $v\simeq 246\,{\rm GeV}$ the electroweak VEV. Note that $\mathcal{O}\left(M_{\rm D}\right)\ll\mathcal{O}\left(M_{\rm R}\right)$ is required to generate the tiny masses for active neutrinos through the seesaw mechanism.

To obtain the interaction between the majoron and the active neutrinos, one can simply take i, j = 1, 2, 3 in eq. (2.4) and identify $n_i \equiv \nu_i$ (for i = 1, 2, 3). Then it follows that $C_{ij} \simeq \delta_{ij}$, where the non-diagonal elements are suppressed by $\mathcal{O}(M_{\rm D}^2/M_{\rm R}^2)$, leading to

$$\mathcal{L}_{J\nu\nu} \simeq \frac{\mathrm{i}J}{2f} \sum_{i=1}^{3} m_i \overline{\nu_i} \gamma_5 \nu_i \,. \tag{2.6}$$

Therefore, the interaction between the majoron and the active neutrinos is approximately diagonal and is suppressed by feeble majoron-neutrino couplings $g_{\nu_i} \equiv m_i/f$.

For the mass region of $1 \text{ eV} \lesssim m_J \lesssim 1 \text{ MeV}$ which will be considered in this work, the majoron can decay to two active neutrinos, where the decay width is given by

$$\Gamma_{J\to 2\nu} = \frac{1}{16\pi f^2} \sum_{i=1}^{3} m_i^2 \sqrt{m_J^2 - 4m_i^2} \simeq \frac{m_J}{16\pi f^2} \sum_{i=1}^{3} m_i^2.$$
 (2.7)

In addition, the majoron can also decay to two photons at two-loop level with the width scaling as [15]

$$\Gamma_{J\to 2\gamma} \sim \alpha^2 \text{Tr} \left(Y_{\nu} Y_{\nu}^{\dagger}\right)^2 m_J^3 / f^2 \,,$$
 (2.8)

where α is the fine-structure constant. The di-photon decay mode is severely constrained by the CMB, X-, gamma- and cosmic-ray observations [12, 13, 15]. In fact, for the low-scale seesaw scenario (i.e., $f \lesssim 100 \,\text{TeV}$) considered in this paper, the Yukawa couplings Y_{ν} are suppressed by the tiny neutrino masses (recall that the seesaw relation gives $Y_{\nu} \sim \sqrt{m_i f}/v \lesssim 10^{-5}$), thereby making $J \to 2\nu$ the dominant decay mode of the majoron.

2.2 Majoron cosmology in the low-scale seesaw scenario

Due to the large hierarchy between m_i and f, the majoron is expected to be long-lived [cf. eq. (2.7)]. For a large enough f, the majoron can naturally serve as a DM candidate [9–17]. For relatively small f, e.g., around the electroweak scale, the majoron becomes unstable within the cosmological time scale and will dominantly decays to active neutrinos.

To see when the majoron decays, let us consider the temperature T_J of nonrelativistic majoron decay, which can be defined as

$$\tau_I^{-1} = \Gamma_J \simeq \Gamma_{J \to 2\nu} \equiv 2H(T_J). \tag{2.9}$$

Here $H(T) \simeq 1.66 \sqrt{g_{\rho}(T)} T^2/M_{\rm Pl}$ is the Hubble parameter at the radiation-dominated epoch, with $g_{\rho}(T)$ the relativistic degrees of freedom for energy density and $M_{\rm Pl} \simeq 1.22 \times 10^{19} \, {\rm GeV}$ the Planck mass. Moreover, the decay width of the majoron Γ_J can be calculated by eq. (2.7) as an approximation. Note that for relativistic majoron decay, the lifetime τ_J in eq. (2.9) is enhanced by an additional Lorentz factor $E_J/m_J > 1$. Combining eqs. (2.7) and (2.9), we obtain that the nonrelativistic decaying temperature T_J scales as

$$T_{J} \simeq 0.077 g_{\rho}^{-1/4} \frac{1}{f} \left(\sum_{i=1}^{3} m_{i}^{2} m_{J} M_{\text{Pl}} \right)^{1/2}$$

$$\simeq 0.997 \left(\frac{3.36}{g_{\rho}} \right)^{1/4} \left(\frac{\sqrt{\sum_{i=1}^{3} m_{i}^{2}}}{0.05 \,\text{eV}} \right) \left(\frac{m_{J}}{0.1 \,\text{MeV}} \right)^{1/2} \left(\frac{f}{100 \,\text{GeV}} \right)^{-1} \,\text{keV} \,, \tag{2.10}$$

where g_{ρ} in the right-handed side of eq. (2.10) should be calculated at T_J . In figure 1, we show the plane of (m_J, f) where the lifetime of the majoron is longer than the age of the Universe $\tau_U \simeq 4.4 \times 10^{17}$ s, and the parameter space where the majoron decays as a nonrelativistic particle (i.e., $T_J < m_J$). We also show the values of m_J and f that lead to the decaying temperature of $T_J = 1\,\mathrm{eV}$ and $T_J = 0.1\,\mathrm{MeV}$, which typically corresponds to the epochs of matter-radiation equality $T_{\rm eq}$ and the completion of the SM neutrino decoupling $T_{\nu,\mathrm{dec}}$, respectively. It can be seen from figure 1 that in the region of nonrelativistic majoron decay with the decaying temperature $T_{\rm eq} \lesssim T_J \lesssim T_{\nu,\mathrm{dec}}$, the corresponding lepton-number breaking scale resides in $f \in [1, 10^5]\,\mathrm{GeV}$ (i.e., the yellow-shaded region in figure 1), which happens to be the low-scale seesaw scenario provided that the masses of RH neutrinos arise from the spontaneous lepton-number violation.

Before calculating the contribution of majoron decay to $N_{\rm eff}$, we need to specify the early evolution of the majoron, which determines the primordial majoron abundance. Generally speaking, there are two possibilities that the majoron can keep thermal equilibrium with SM particles in the early Universe:

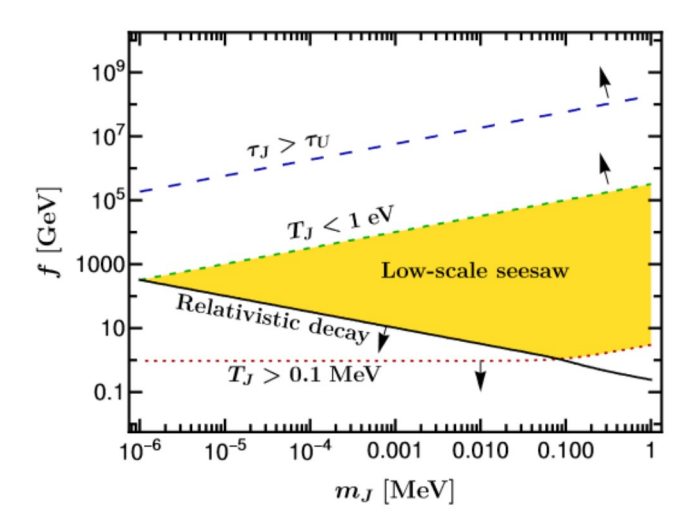


Figure 1. The decaying temperature of the majoron T_J with different values of the majoron mass m_J and the lepton-number breaking scale f. Some typical epochs of the majoron decay are shown in the plot where: the majoron is stable over the cosmological time scale $\tau_U \simeq 4.4 \times 10^{17}$ s (above the blue long-dashed line), the majoron decays after the epoch of the matter-radiation equality $T_{\rm eq} \simeq 1\,{\rm eV}$ (above the green short-dashed line), the majoron decays before the SM neutrino decoupling epoch $T_{\nu,{\rm dec}} \simeq 0.1\,{\rm MeV}$ (below the red dotted line), and the majoron decays as a relativistic particle (below the black solid line). The yellow-shaded region is the parameter space which interests us in this work, i.e., the majoron decays nonrelativistically with the decaying temperature $T_{\rm eq} \lesssim T_J \lesssim T_{\nu,{\rm dec}}$. The lepton-number breaking scale in the yellow-shaded region resides in $1\,{\rm GeV} \lesssim f \lesssim 100\,{\rm TeV}$, which corresponds to the low-scale seesaw scenario.

• First, the RH neutrinos can readily be thermalized in the SM plasma via two-body/inverse decay or rapid active-neutrino oscillations [32, 33]. Before the electroweak gauge symmetry breaking, the majoron couples to RH neutrinos via

$$\mathcal{L}_{JNN} = -\frac{\mathrm{i}J}{2\sqrt{2}}\overline{N_{\mathrm{R}}^{c}}Y_{N}N_{\mathrm{R}} + \text{h.c.} = -\frac{\mathrm{i}J}{2f}\sum_{i=1}^{3}M_{i}\overline{N_{i}}\gamma_{5}N_{i}, \qquad (2.11)$$

where the mass eigenstates of the RH neutrinos $N_{\rm R} + N_{\rm R}^c \equiv (N_1, N_2, N_3)^{\rm T}$ have been defined, and M_i is the mass of N_i . Furthermore, for Yukawa couplings Y_N that are not too small, the scattering $2N \to 2J$ via eq. (2.11) can in turn thermalize the majoron for the temperature $T \gtrsim M_i$. Note that there is no decaying channel of $N_i \to N_j + J$ (with $M_i > M_j$) since the non-diagonal elements in Y_N are not physical before the gauge symmetry breaking.

• Second, the majoron can couple with the Higgs boson via the following interaction

$$V \supset \lambda_{\Phi S} \left(\Phi^{\dagger} \Phi \right) \left(S^{\dagger} S \right), \tag{2.12}$$

which is not forbidden by the global U(1)_L symmetry and should be included into a general scalar potential (see appendix A.2 for more details). Moreover, it was shown [34] that even for a portal coupling $\lambda_{\Phi S}$ as small as $\mathcal{O}(10^{-6})$, the scattering $2\Phi \to 2S$ can

still thermalize the scalar S. After the gauge symmetry breaking, the majoron couples with the SM Higgs boson h through the mixing (induced by $\lambda_{\Phi S}$) between two CP-even bosons h and ρ , and can be thermalized via $h \to 2J$ or $2h \to 2J$.

Therefore, a thermalized majoron in the early Universe can easily be realized in the minimal setup that exhibits a spontaneous global U(1)_L breaking in the scalar sector and at the same time, predicts an unstable majoron decaying at $T_{\rm eq} \lesssim T_J \lesssim T_{\nu, \rm dec}$. Since the majoron is much lighter than the RH neutrinos and the Higgs bosons, it is expected to undergo relativistic freeze-out. The freeze-out temperature $T_{\rm fo}$ of the majoron depends on the details of the UV models, and will be treated as an input parameter in the following discussions.

After the gauge symmetry breaking, the active neutrinos can also generate the majoron abundance through the neutrino coalescence process $2\nu \to J$ [cf. eq. (2.6)]. Due to the suppression of the majoron-neutrino coupling $g_{\nu_i} \equiv m_i/f$, the production channel follows the freeze-in evolution [35–38] and culminates at $T \simeq \mathcal{O}(m_J)$. Therefore, the majoron abundance is, strictly speaking, not a constant after the relativistic freeze-out. As can be seen in figure 1, for $1 \text{ eV} \lesssim m_J \lesssim 1 \text{ MeV}$ and a suppressed coupling g_{ν_i} , the majoron is expected to decay after the SM neutrino decoupling. This late-time decay will modify the effective number of neutrino species N_{eff} due to the energy injection to active neutrinos. Such effects have been studied in refs. [26–30] where the constraints of N_{eff} from the CMB measurements have been applied to derive the upper bound of the majoron-neutrino coupling in terms of the majoron mass.

Nevertheless, previous studies have mainly focused on the majoron-neutrino effective interaction, where the majoron abundance is generated by and then depleted back to the SM neutrinos.³ It is the purpose of this work to detail the effects of the primordial abundance on $N_{\rm eff}$. While we concentrate on the low-scale seesaw scenario, it is worthwhile to emphasize that the analysis performed in subsequent sections can analogously be applied to other UV scenarios, where a new light particle coupling to active neutrinos or photons has a non-negligible primordial abundance before the SM neutrino decoupling and decays after that epoch.

3 Analytical derivation of $\Delta N_{\rm eff}$ from majoron decay

In this section, we perform an approximate analytical calculation of the $N_{\rm eff}$ excess from majoron decay (i.e., $\Delta N_{\rm eff} \equiv N_{\rm eff} - N_{\rm eff}^{\rm SM}$) by assuming that the majoron decays instantaneously, where $N_{\rm eff}^{\rm SM} \simeq 3.045$ denotes the SM prediction of the effective number of neutrino species [39–46]. The calculation depends on the kinematic properties (that is, relativistic or nonrelativistic) of the majoron at decay. In the first two subsections, we compute $\Delta N_{\rm eff}$ from relativistic and nonrelativistic majoron decay respectively, with the primordial majoron abundance inherited from the relativistic freeze-out. In the last two subsections, we compute $\Delta N_{\rm eff}$ from the freeze-in production followed by majoron decay, where there is no primordial majoron abundance.

 $^{^3}$ See, however, refs. [28–30] that partly discussed a primordial majoron abundance.

3.1 Relativistic freeze-out and relativistic decay

In order to be model-independent, we do not specify the freeze-out process of the majoron from UV scenarios (i.e., the majoron will be thermalized via the scattering either with the RH neutrinos or with the Higgs boson); rather, we treat the freeze-out temperature $T_{\rm fo}$ as an input parameter. Then the yield of the majoron at $T_{\rm fo}$ is given by

$$Y_{J,\text{fo}}^n \equiv \frac{n_J}{s_{\text{SM}}} \Big|_{T=T_{\text{fo}}} = \frac{45\zeta(3)}{2\pi^4 g_s(T_{\text{fo}})},$$
 (3.1)

where $n_J = \zeta(3)T^3/\pi^2$ is the number density of the relativistic majoron in thermal equilibrium with $\zeta(x)$ the Riemann ζ -function, and $s_{\rm SM}$ is the SM entropy density

$$s_{\rm SM} = g_s(T) \frac{2\pi^2}{45} T^3 \,, \tag{3.2}$$

with $g_s(T)$ the relativistic degrees of freedom for entropy in the SM. Therefore, the majoron freeze-out yield depends only on the relativistic degrees of freedom at T_{fo} .

The observations of the light-element abundances generated during the BBN era put stringent constraints on the interactions of neutrinophilic particles [47, 48]. Here we would like to estimate the contribution of the majoron to $N_{\rm eff}$ at the BBN epoch. It is usually stated that the BBN process starts after the deuterium bottleneck temperature $T \simeq 0.078\,{\rm MeV}$ [49–51]. Nevertheless, any extra radiation before the neutron-proton freeze-out at $T \simeq 0.8\,{\rm MeV}$ will modify the Hubble expansion rate, leading to more neutron abundance at freeze-out and hence more ⁴He. Observations of the primordial helium-4 synthesized at the BBN epoch will constrain the extra radiation, which is effectively parametrized by $\Delta N_{\rm eff}$ [51]. If the majoron decays after $T \simeq 0.1\,{\rm MeV}$, the majoron itself contributes to the Hubble expansion rate before the BBN starts. Then $\Delta N_{\rm eff}$ at the BBN epoch can be approximated by ⁴

$$\Delta N_{\text{eff}}^{\text{BBN}} = \frac{\rho_J}{\rho_{\nu}^{\text{SM}}} \Big|_{T = T_{\text{BBN}}} = \frac{\rho_J (T_{\text{fo}})}{\rho_{\nu}^{\text{SM}} (T_{\text{BBN}})} \left[\frac{s_{\text{SM}} (T_{\text{BBN}})}{s_{\text{SM}} (T_{\text{fo}})} \right]^{4/3} = \frac{4}{7} \left(\frac{g_{s,\text{BBN}}}{g_{s,\text{fo}}} \right)^{4/3}, \quad (3.3)$$

where $g_{s,BBN}$ and $g_{s,fo}$ denote the relativistic degrees of freedom at T_{BBN} and T_{fo} , respectively, and

$$\rho_{\nu}^{\text{SM}} = \frac{7}{4} \frac{\pi^2}{30} T_{\nu}^4 \,, \tag{3.4}$$

is the one-flavor neutrino energy density with $T_{\nu}=T_{\gamma}$ before neutrino decoupling. For definiteness, we will take $T_{\rm BBN}\simeq 1\,{\rm MeV}$ to denote the temperature before the neutron-proton freeze-out.

Next, let us consider the situation where the majoron decays relativistically after the BBN ends and prior to the matter-radiation equality epoch $T_{\rm eq} \simeq 1\,{\rm eV}$. The energy from the majoron would then inject into active neutrinos, acting as extra radiation at the recombination

⁴Note that the quantity $\rho_J/s_{\rm SM}^{4/3}$ is a constant after the majoron decouples. In addition, the majoron abundance from the freeze-in neutrino coalescence $2\nu \to J$ contributes negligibly to the majoron abundance and $N_{\rm eff}$ when the majoron is still in the relativistic regime.

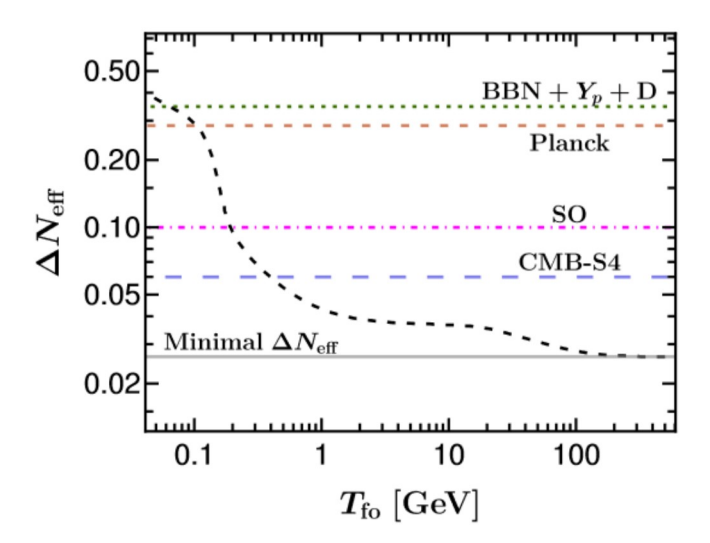


Figure 2. $\Delta N_{\rm eff}$ calculated from relativistic majoron decay at the epochs of BBN or CMB with different freeze-out temperature $T_{\rm fo}$ (black short-dashed line). The regions above different horizontal lines correspond to the 2σ excluded regions of $\Delta N_{\rm eff}$ from the constraints of BBN+ Y_p +D (green dotted line), Planck (red short-dashed line), as well as the future projected sensitivities of SO (magenta dot-dashed line) and CMB-S4 (blue dashed line). The gray solid line denotes the minimal $\Delta N_{\rm eff} \simeq 0.027$, which corresponds to the freeze-out temperature $T_{\rm fo} \gtrsim \mathcal{O}(100)~{\rm GeV}$.

epoch $T \simeq 0.1\,\mathrm{eV}$ and being constrained by the CMB measurement. In the approximation of instantaneous decay, we arrive at

$$\Delta N_{\text{eff}}^{\text{CMB}} = \frac{\rho_{J \to 2\nu}}{\rho_{\nu}^{\text{SM}}} \bigg|_{T = T_{\text{eq}}} = \frac{4}{7} \left(\frac{11}{4}\right)^{4/3} \left(\frac{g_{s,\text{CMB}}}{g_{s,\text{fo}}}\right)^{4/3}, \tag{3.5}$$

where $\rho_{J\to 2\nu}$ denotes the neutrino energy density inherited from relativistic majoron decay, and the factor $T_{\nu}/T_{\gamma} = (4/11)^{1/3}$ has been used for the (instantaneous) neutrino decoupling. In addition, we have assumed that the decay is completed before $T_{\rm eq}$ so that $\Delta N_{\rm eff}$ is evaluated at $T_{\rm eq}$.

Given $g_{s,\mathrm{BBN}}/g_{s,\mathrm{CMB}}=11/4,^5$ we arrive at $\Delta N_{\mathrm{eff}}^{\mathrm{BBN}}=\Delta N_{\mathrm{eff}}^{\mathrm{CMB}}$. This identity implies that when the majoron decays in the relativistic regime, the extra radiation contributes equally to N_{eff} at the epochs of BBN and CMB, which only depends on the freeze-out temperature. It is clear that a lower T_{fo} leads to a larger ΔN_{eff} . This can be understood as follows. After the relativistic freeze-out of the majoron, the decoupling of other SM particles will inject energies into the plasma of photons and neutrinos, thereby reheating the SM bath and enhancing ρ_{ν}^{SM} . Therefore, the later the majoron decouples, the less enhancement ρ_{ν}^{SM} will receive, which implies a larger ΔN_{eff} .

In figure 2, we show the behavior of $\Delta N_{\rm eff}$ calculated from relativistic majoron decay at the epochs of BBN or CMB with different freeze-out temperatures $T_{\rm fo}$, where the evolution of $g_s(T)$ is taken from ref. [52]. We also show the constraints on $\Delta N_{\rm eff}$ from the Planck

⁵This ratio is obtained in the approximation of instantaneous neutrino decoupling, which is sufficient for the analytic analysis.

2018 result [1]: $N_{\rm eff} = 2.99 \pm 0.17$, the combination of BBN, helium (Y_p) and deuterium (D) abundances [2]: $N_{\rm eff} = 2.889 \pm 0.229$, and from the future sensitivities of Simon Observatory (SO) [22, 23] and CMB-S4 [24, 25]. The 2σ upper bounds are given by

Planck:
$$\Delta N_{\text{eff}} < 0.285$$
, (3.6)

BBN +
$$Y_p$$
 + D : $\Delta N_{\text{eff}} < 0.347$, (3.7)

$$SO: \Delta N_{\text{eff}} < 0.1, \tag{3.8}$$

CMB-S4:
$$\Delta N_{\text{eff}} < 0.06$$
. (3.9)

It can be seen that for the majoron that decays relativistically after the neutrino decoupling and before the matter-radiation equality epoch, the current constraints from BBN+ Y_p +D and Planck requires $T_{\rm fo} > 64\,{\rm MeV}$ and $T_{\rm fo} > 104\,{\rm MeV}$, respectively, while the future sensitivities from the SO and CMB-S4 will further limit the decoupling temperature to $T_{\rm fo} > 192\,{\rm MeV}$ and $T_{\rm fo} > 397\,{\rm MeV}$, respectively. Note that a minimal $\Delta N_{\rm eff} \simeq 0.027$ is expected for the early-time decoupling of the majoron, i.e., $T_{\rm fo} \gtrsim \mathcal{O}(100)\,{\rm GeV}$, where all the SM particles are relativistic with $g_{\rm s,fo} = 106.75$.

3.2 Relativistic freeze-out and nonrelativistic decay

Now let us turn to the more interesting scenario, where the majoron decays in the nonrelativistic regime. We expect that $\Delta N_{\rm eff}^{\rm BBN} \neq \Delta N_{\rm eff}^{\rm CMB}$ in this case. The former is still given by eq. (3.3) while the latter is calculated as

$$\Delta N_{\text{eff}}^{\text{CMB}} = \frac{\rho_{J \to 2\nu}}{\rho_{\nu}^{\text{SM}}} \bigg|_{T = T_{\text{eq}}} \simeq \frac{m_J Y_{J,\text{fo}}^n s_{\text{SM}}}{\rho_{\nu}^{\text{SM}}} \bigg|_{T = T_J} \simeq 0.815 \left(\frac{g_{s,T_J}}{g_{s,\text{fo}}}\right) \left(\frac{m_J}{T_J}\right), \quad (3.10)$$

where the energy injection from the majoron into neutrinos at $T_{\rm eq}$ is estimated by the value of $m_J n_J$ at T_J [defined in eq. (2.9)]. Note that we do not include the contribution to the majoron abundance from the freeze-in process $2\nu \to J$, so the yield Y_I^n keeps constant after freeze-out.

From eq. (3.10) it is clear that later decay of the majoron will cause a larger $\Delta N_{\rm eff}$ at the CMB epoch. This can also be understood by the dilution-resistant effect [30] (see section 3.4 for more discussions): after the decoupling of neutrinos, we have $\rho_{\nu}^{\rm SM} \propto a^{-4}$ with a the scale factor, while the majoron energy density in the nonrelativistic regime scales as $\rho_J \propto a^{-3}$. As a result, later decay of the majoron implies that $\rho_{\nu}^{\rm SM}$ suffers from more redshift (dilution) than the energy of the nonrelativistic majoron ρ_J (resistance), thereby leading to a larger $\Delta N_{\rm eff}$ after majoron decay.

A key observation is that, since later decay of the majoron implies a larger lepton-number breaking scale f or equivalently a smaller majoron-neutrino coupling, and leads to a larger $\Delta N_{\rm eff}^{\rm CMB}$, it implies that the constraint from $\Delta N_{\rm eff}^{\rm CMB}$ will put an upper bound on f. This is in contrast to the freeze-in scenario without a primordial majoron abundance, where a lower bound of f can be obtained from the constraint of $\Delta N_{\rm eff}^{\rm CMB}$, as we shall discuss below.

3.3 Freeze-in without primordial majoron

In the low-scale seesaw scenario, where f is around the electroweak scale, the neutrino coalescence $2\nu \to J$ can also contribute to the majoron abundance via the freeze-in mechanism.

In this subsection, we calculate the excess of $N_{\rm eff}$ from freeze-in production of the majoron, and make a comparison with the results derived in the previous subsection with a primordial majoron abundance.

To simplify the calculation of $\Delta N_{\rm eff}$, we assume that the freeze-in production of the majoron is essentially completed before it decays. We first consider the case of nonrelativistic majoron decay. The Boltzmann equation of the majoron abundance before decay is given by

$$\frac{\mathrm{d}Y_{J,\mathrm{fi}}^n}{\mathrm{d}T} = -\frac{\mathcal{C}_{2\nu\to J}^n}{s_{\mathrm{SM}}HT},\tag{3.11}$$

where $Y_{J,\text{fi}}^n \equiv n_J/s_{\text{SM}}$ denotes the freeze-in abundance of the majoron and the collision term $\mathcal{C}_{2\nu\to J}^n$ is computed in appendix B, which is a function of the neutrino temperature T_{ν} .

Let us assume again that the decay occurs instantaneously at T_J after the neutrino decoupling. Then the excess of $N_{\rm eff}$ at the CMB epoch coming from the nonrelativistic majoron decay can be calculated by

$$\Delta N_{\rm eff}^{\rm CMB} \simeq \left. \frac{m_J Y_{J,\rm fi}^n s_{\rm SM}}{\rho_{\nu}^{\rm SM}} \right|_{T=T_J} \simeq 2.94 g_{s,T_J} Y_{J,\rm fi}^n \left(\frac{m_J}{T_J} \right), \tag{3.12}$$

where g_{s,T_J} denotes the relativistic degrees of freedom at the decaying temperature. Note that the nonrelativistic factor $m_J/T_J \propto \sqrt{m_J/M_{\rm Pl}}f/m_i$ [cf. eq. (2.10)] also appears here as in eq. (3.10).

At first sight, it seems that a heavier majoron and a larger lepton-number breaking scale lead to a larger $\Delta N_{\rm eff}^{\rm CMB}$, which occurs in the freeze-out case (see section 3.2). However, $\Delta N_{\rm eff}^{\rm CMB}$ in eq. (3.12) also depends on m_J and f through $Y_{J,{\rm fi}}^n$. To see it more clearly, we calculate $Y_{J,{\rm fi}}^n$ with the following approximations:

- We take the Boltzmann approximation of the neutrino distribution functions so that the collision term $C_{2\nu\to J}^n$ is given by eq. (B.6).
- We assume that neutrinos decouple instantaneously at $T_{\nu,\text{dec}} \simeq 0.1 \text{ MeV}$, so the neutrino temperature in $C_{2\nu\to J}^n$ is given by $T_{\nu} = T$ (for $T > T_{\nu,\text{dec}}$) or $T_{\nu}/T = (4/11)^{1/3}$ (for $T < T_{\nu,\text{dec}}$).
- To obtain the freeze-in abundance of the majoron, one needs to integrate eq. (3.12) over the temperature. Since the majoron decays nonrelativistically after the neutrino decoupling, we can further expand the collision term in the integral in terms of m_J/T for $T > T_{\nu,\text{dec}}$ and in terms of T/m_J for $T < T_{\nu,\text{dec}}$.

With above approximations, we arrive at a very simple result

$$\Delta N_{\rm eff}^{\rm CMB} \simeq 0.139 \left(\frac{{\rm MeV}}{m_J}\right)^{1/2} \left(\frac{{\rm GeV}}{f}\right),$$
 (3.13)

where $g_{s,T_J} \simeq 3.36$ has been used, and for concreteness, we have taken the normal ordering of the neutrino masses with $m_1 = 0$ and $\sum_{i=1}^{3} m_i^2 \simeq (0.0086 \,\text{eV})^2 + (0.05 \,\text{eV})^2$ [53].

From eq. (3.13) it is now clear that for the freeze-in case, a lighter majoron and a smaller f will lead to a larger $\Delta N_{\rm eff}$. Therefore, the constraint from CMB measurements will put a lower bound on the lepton-number breaking scale. This is in contrast to the case of freeze-out with a primordial majoron abundance, as already discussed in section 3.2.

3.4 Comparison between freeze-out and freeze-in

From eq. (3.13), one may naively expect that $\Delta N_{\rm eff}$ can keep increasing with the decreasing of m_J and f. However, a lighter majoron and a larger coupling (i.e., a smaller f) would make the majoron-neutrino system easier to reach thermal equilibrium, when the freeze-in formalism and consequently the result in eq. (3.13) are no longer applicable. In fact, as pointed out in refs. [30, 42], when the majoron gets thermalized with the SM neutrinos, one obtains a maximal $\Delta N_{\rm eff} \simeq 0.12$.

Based on the analysis in section 3.3, we can understand the maximal $\Delta N_{\rm eff}$ in a different way.⁶ Recall that the result in eq. (3.13) is derived in the regime of nonrelativistic majoron decay, i.e., $p_J < m_J$ with p_J the magnitude of the majoron momentum. The averaged momentum for a nonrelativistic thermalized majoron is given by $\langle p_J \rangle \simeq \sqrt{3m_J T_J}$.⁷ By requiring $\langle p_J \rangle < m_J$ and taking advantage of eq. (2.10), we obtain a lower bound on f:

$$\left(\frac{f}{\text{GeV}}\right) \gtrsim 0.96 \left(\frac{\text{MeV}}{m_J}\right)^{1/2},$$
 (3.14)

where $\sum_{i=1}^{3} m_i^2 \simeq (0.0086\,\mathrm{eV})^2 + (0.05\,\mathrm{eV})^2$ and $g_\rho(T_J) \simeq 3.36$ have been used. Substituting eq. (3.14) back to eq. (3.13), we arrive at $\Delta N_{\mathrm{eff}}^{\mathrm{CMB}} \lesssim 0.14$. This confirms the result in refs. [30, 42] that nonrelativistic majoron decay from the freeze-in mechanism without a primordial abundance can lead to a maximal ΔN_{eff} at $\mathcal{O}(0.1)$.

Another point worth mentioning is that there is no excess of $N_{\rm eff}$ from the relativistic majoron decay in the freeze-in scenario. In section 3.1, we have demonstrated that the relativistic majoron decay with a primordial abundance can generate a nonzero $\Delta N_{\rm eff}$. However, this is not the case if the majoron abundance only comes from the freeze-in production, which instead predicts a vanishing $\Delta N_{\rm eff}$. To see it more clearly, we can rewrite the Boltzmann equation of the majoron-neutrino system as [30]

$$\frac{\mathrm{d}}{\mathrm{d}a} \left[(\rho_J + \rho_\nu) a^4 \right] = a^3 (\rho_J - 3P_J) \,, \tag{3.15}$$

where P_J denotes the pressure of the majoron. In the relativistic regime, we have $P_J = \rho_J/3$, so the comoving energy density $(\rho_J + \rho_\nu) a^4$ is a constant. In this case, if there is no primordial majoron abundance, the energy density will first transfer from neutrinos to the majoron through the freeze-in process $2\nu \to J$ and then back to neutrinos through the relativistic majoron decay $J \to 2\nu$, while the total energy density of the majoron-neutrino system in a comoving volume remains unchanged. Therefore, there would be no excess of $N_{\rm eff}$ if the majoron decays in the relativistic regime.

In conclusion, if there is no primordial majoron abundance, a nonzero $\Delta N_{\rm eff}$ can only be generated if the majoron decays in the nonrelativistic regime. In addition, a smaller lepton-number breaking scale f and majoron mass m_J lead to a larger $\Delta N_{\rm eff}$, which has a maximal value at $\mathcal{O}(0.1)$. On the other hand, when there is a primordial majoron abundance,

 $^{^6}$ In refs. [30, 42], the maximal $\Delta N_{\rm eff}$ is derived from the conservation of particle number, energy and entropy.

⁷Strictly speaking, the majoron never reaches thermal equilibrium in our analysis of the freeze-in process. Nevertheless, here we use the statistics for a thermalized majoron since we only want to estimate the upper bound of ΔN_{eff} that is caused by the majoron decay.

both the relativistic and nonrelativistic majoron decay at late times can generate a nonzero $\Delta N_{\rm eff}$. In particular, for the case of nonrelativistic decay, a larger f and m_J will predict a larger $\Delta N_{\rm eff}$, contrary to the freeze-in case where there is no primordial abundance. To have a more precise constraint on the lepton-number breaking scale from observations of $N_{\rm eff}$, in the next section, we proceed to perform a stricter calculation of $\Delta N_{\rm eff}$ in the nonrelativistic region by going beyond the approximation of instantaneous majoron decay used in section 3.2.

4 Calculation of $\Delta N_{\rm eff}$ beyond instantaneous majoron decay

In this section, we carry out a stricter calculation of $\Delta N_{\rm eff}$ from nonrelativistic majoron decay, which has a primordial abundance inherited from the relativistic freeze-out. We also make a comparison with the freeze-in production $2\nu \to J$ followed by nonrelativistic decay $J \to 2\nu$. For later reference, we use the following shorthand:

 $\begin{aligned} & FONR \equiv relativistic \ Freeze-Out + NonRelativistic \ decay \,, \\ & FINR \equiv Freeze-In + NonRelativistic \ decay \,. \end{aligned}$

We are interested in the case where the majoron decays after the SM neutrinos have decoupled from the plasma at around $T_{\nu, \rm dec} \simeq 0.1\,\mathrm{MeV}$ [41–46, 54], so as to suppress the nontrivial impacts on the BBN processes as well as the neutrino decoupling. Under this circumstance, the neutrinos generated from majoron decay at temperatures below $T_{\nu, \rm dec}$ can no longer be thermalized via the SM weak interactions. Therefore, in the FONR case, we can treat majoron decay separately from the SM thermal bath.

In general, the neutrino coalescence $2\nu \to J$ also contributes to $\Delta N_{\rm eff}$ in the FONR case. Nevertheless, we will neglect it in the calculation of $\Delta N_{\rm eff}$ for two reasons. First, as shown in section 3.4, the contribution from neutrino coalescence to $\Delta N_{\rm eff}$ can only reach up to $\mathcal{O}(0.1)$, which is beyond the sensitivity of current CMB measurements [1]. Second, as can be seen from section 3.2 and section 3.3, the dependence of $\Delta N_{\rm eff}$ on m_J and f is opposite between the FONR and the FINR cases, so it would be more clear to treat the two processes separately. The inclusion of neutrino coalescence in the FONR case will be discussed in section 5.

Without including the contribution from neutrino coalescence, the Boltzmann equations governing the nonrelativistic majoron decay are given by

$$\frac{\mathrm{d}\rho_J}{\mathrm{d}t} + 3H\rho_J = -\mathcal{C}_{J\to 2\nu}^{\rho}, \quad \frac{\mathrm{d}\rho_\nu}{\mathrm{d}t} + 4H\rho_\nu = \mathcal{C}_{J\to 2\nu}^{\rho}, \tag{4.1}$$

where $C_{J\to 2\nu}^{\rho}$ is the collision term responsible for the energy transfer rate. In the nonrelativistic regime, we have $C_{J\to 2\nu}^{\rho} \simeq m_J n_J \Gamma_J$ with $\Gamma_J \simeq \Gamma_{J\to 2\nu}$ and the primordial majoron abundance $n_J = \zeta(3)T^3/\pi^2$ coming from relativistic freeze-out.

Defining $Y_J^n \equiv n_J/s_{\rm SM} = \rho_J/\left(m_J s_{\rm SM}\right)$ and $Y_\nu^\rho \equiv \rho_\nu/s_{\rm SM}^{4/3}$, we can rewrite the Boltzmann equations as

$$\frac{\mathrm{d}Y_J^n}{\mathrm{d}T} = \frac{\Gamma_J Y_J^n}{HT}, \qquad \frac{\mathrm{d}Y_\nu^\rho}{\mathrm{d}T} = -\frac{m_J \Gamma_J Y_J^n}{s_{\mathrm{SM}}^{1/3} HT}, \tag{4.2}$$

$T_{ m fo}/{ m MeV}$	64	104	192	397	$> \mathcal{O}(10^5)$		
$Y_{J,\mathrm{ini}}^n$	0.018	0.015	0.007	0.005	0.003	9×10^{-4}	3×10^{-4}
$\Delta N_{ m eff}^{ m BBN}$	0.347	0.285	0.100	0.060	0.027	0.008	0.003

Table 1. Correspondence among the freeze-out temperatures T_{fo} , the primordial majoron abundances $Y_{L\text{inj}}^n$, and the contributions to ΔN_{eff} at the BBN epoch.

which lead to the solutions

$$Y_J^n(T) = Y_{J,\text{ini}}^n e^{-\frac{\Gamma_J}{2} \left(H^{-1} - H_{\text{ini}}^{-1}\right)}, \qquad Y_{\nu}^{\rho}(T) = m_J \Gamma_J \int_T^{T_{\text{ini}}} dT' \frac{Y_J^n(T')}{s_{\text{SM}}^{1/3} H T'}, \tag{4.3}$$

with an initial temperature $T_{\rm ini} \gg T_J$ and $H_{\rm ini} \equiv H(T_{\rm ini})$. For definiteness, we take $T_{\rm ini} = 0.1$ MeV, which is consistent with the requirement of $T_J \lesssim T_{\nu, \rm dec}$. It should be pointed out that a higher $T_{\rm ini}$ does not modify the result significantly, since the decay mainly occurs around T_J determined by $\Gamma_J \simeq 2H(T_J)$, and Y_J^n is exponentially suppressed for $T < T_J$. In addition, the initial abundance is determined by the freeze-out abundance in eq. (3.1), i.e.,

$$Y_{J,\text{ini}}^n = Y_{J,\text{fo}}^n = \frac{45\zeta(3)}{2\pi^4 g_s(T_{\text{fo}})}.$$
 (4.4)

In table 1, we have listed the correspondence between $T_{\rm fo}$ and $Y_{J,\rm ini}^n$ for some typical freeze-out temperatures. Alternatively, one can also use the contribution of the relativistic majoron to $\Delta N_{\rm eff}$ at the BBN epoch to characterize the primordial abundance (i.e., the third line of table 1). Note that the first five values of $\Delta N_{\rm eff}^{\rm BBN}$ in table 1 can be obtained from $T_{\rm fo}$ using eq. (3.3). For $\Delta N_{\rm eff}^{\rm BBN} < 0.027$, it cannot be inherited from the relativistic freeze-out mechanism, where the thermal plasma at $T > \mathcal{O}(100)$ GeV only contains the SM degrees of freedom. Nevertheless, we can still establish a one-to-one correspondence between $\Delta N_{\rm eff}^{\rm BBN}$ and the primordial majoron abundance $Y_{J,\rm ini}^n$.

Since the nonrelativistic majoron decay occurs after the neutrino decoupling and before the matter-radiation equality epoch, when the relativistic species include photons and neutrinos, it is reasonable to treat the relativistic degrees of freedom g_{ρ} (in the Hubble parameter) and g_s (in the entropy density) as constants. Taking into account the temperature ratio between photons and neutrinos derived from noninstantaneous neutrino decoupling: $T/T_{\nu} \simeq 1.3985$ [42], one obtains

$$g_{\rho} \simeq 2 + \frac{7}{8} \times 2 \times 3 \times \left(\frac{T_{\nu}}{T}\right)^4 \simeq 3.38,$$
 (4.5)

$$g_s \simeq 2 + \frac{7}{8} \times 2 \times 3 \times \left(\frac{T_\nu}{T}\right)^3 \simeq 3.93.$$
 (4.6)

Combining eqs. (4.3)–(4.6) and given a freeze-out temperature $T_{\rm fo}$, one can obtain the neutrino energy density Y_{ν}^{ρ} that comes from the majoron decay. The excess of $N_{\rm eff}$ at the

⁸This exponential suppression also justifies the approximate analytical results derived in section 3 under the approximation of instantaneous majoron decay.

CMB epoch is then given by

$$\Delta N_{\text{eff}}^{\text{CMB}} = \frac{Y_{\nu}^{\rho} s_{\text{SM}}^{4/3}}{\rho_{\nu}^{\text{SM}}} \bigg|_{T=T_{\text{eq}}}.$$
(4.7)

Note that $\Delta N_{\rm eff}$ calculated above is based on eq. (4.1), where only the contribution from majoron decay $J \to 2\nu$ is included. On the other hand, the heavy sterile neutrinos N_i could also contribute to $\Delta N_{\rm eff}$ through decay $(N_i \to J + \nu_j)$ or 2-to-2 scattering $(2J \to 2\nu)$ mediated by N_i). In the following, we show that the contributions from sterile neutrinos to $\Delta N_{\rm eff}$ are negligible compared with that from majoron decay.

- We first consider the contribution from sterile neutrino decay $N_i \to J + \nu_j$ (for i, j = 1, 2, 3). Since the masses of sterile neutrinos satisfy $M_i \sim f \gg T_{\nu, \text{dec}}$, the decay occurs much earlier than the decoupling of active neutrinos. So the direct contribution from decay to ΔN_{eff} is washed out as active neutrinos are still in thermal equilibrium with photons. On the other hand, the freeze-in production of majoron abundance from N_i decay culminates at $T \simeq \mathcal{O}(M_i)$, at which the relativistic majoron freeze-out also takes place. At this epoch, the contribution to primordial majoron abundance is dominated by the thermal freeze-out, while the freeze-in contribution is negligible.
- Next we consider the contribution from $2J \to 2\nu$ mediated by N_i (for i=1,2,3). We can compute the cross section of $2J \to 2\nu$ using eq. (A.17), with the coupling suppressed by $C_{ij} \sim Y_{\nu} \lesssim 10^{-5}$ in the low-scale seesaw scenario. The cross section is s-wave dominated, so that we can estimate the collision term as follow:

$$C_{2J\to2\nu}^{\rho} \sim \langle \sigma v \rangle_{2J\to2\nu} n_J^2 m_J \sim \frac{m_J n_J^2}{f^4} \sum_{i=1}^3 m_i^2.$$
 (4.8)

Here we have neglected the exact numerical factor from phase-space integration, which is smaller than that from majoron decay. Recall that the collison term from majoron decay is given by $\mathcal{C}_{J\to 2\nu}^{\rho} = m_J n_J \Gamma_J$. So we obtain $\mathcal{C}_{J\to 2\nu}^{\rho}/\mathcal{C}_{2J\to 2\nu}^{\rho} \sim m_J f^2/T^3$. Given $m_J \gtrsim T$ for nonrelativistic majoron decay/annihilation and $f \gg m_J$, we conclude that the contribution to $\Delta N_{\rm eff}$ from majoron annihilation $2J \to 2\nu$ is strongly suppressed compared with that from majoron decay $J \to 2\nu$.

Based on our calculations of $\Delta N_{\rm eff}$ discussed above, the excluded regions in the (m_J, f) plane from the current CMB measurements are shown in figure 3. To compare the calculation of $\Delta N_{\rm eff}$ using the approximation of instantaneous majoron decay in section 3.2 with non-instantaneous decay in section 4, we have shown the excluded regions obtained from both in figure 3, which match quite well with each other. Therefore, the instantaneous majoron decay serves as a good approximation in our problem.

The excess of $N_{\rm eff}$ from the majoron decay depends on the primordial majoron abundance, which is characterized by the freeze-out temperature $T_{\rm fo}$ in eq. (4.4). In figure 3, we have shown results from two typical freeze-out temperatures: $T_{\rm fo} = 64\,{\rm MeV}$ and $T_{\rm fo} > 100\,{\rm GeV}$. The first one is the lowest freeze-out temperature that is allowed by BBN+ Y_p +D (see figure 2). A lower $T_{\rm fo}$ corresponds to a larger primordial abundance and would lead to a

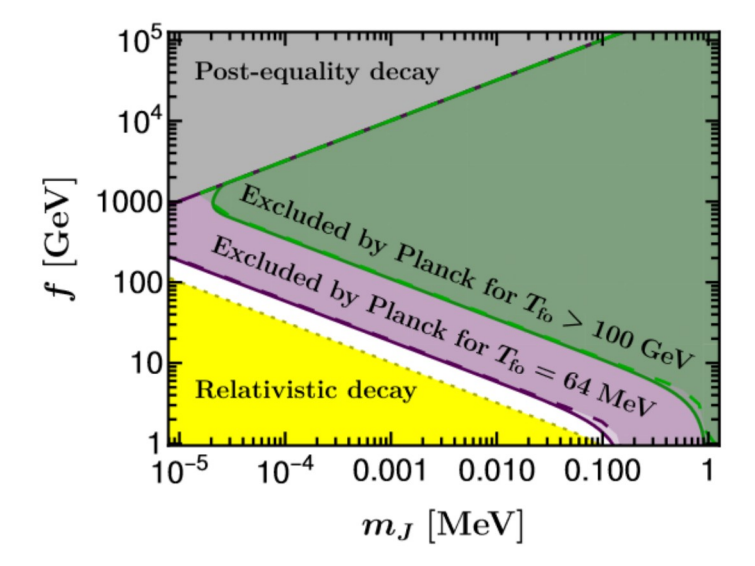


Figure 3. Allowed parameter space of the majoron mass m_J and the lepton-number breaking scale f under the constraints of current CMB measurements on N_{eff} . The pink- and green-shaded regions in the upper right corner are excluded by Planck 2018 at 2σ level [1], with different primordial majoron abundances characterized by the freeze-out temperatures T_{fo} . The excluded regions are obtained from instantaneous decay in section 3.2 (dashed line) and noninstantaneous decay in section 4 (solid line), respectively. In addition, the yellow-shaded region in the lower left corner corresponds to the relativistic decay regime, while the gray-shaded region in the upper left corner corresponds to the scenario where the majoron decays after the matter-radiation equality epoch (post-equality decay).

larger $\Delta N_{\rm eff}$ excluded by the BBN measurements [cf. eq. (3.3)]. The second one is the case where the freeze-out temperature is sufficiently high and all the SM species are relativistic, corresponding to a minimal $\Delta N_{\rm eff} \simeq 0.027$ at the BBN epoch. We can see that for the largest primordial abundance allowed by current BBN measurements, the majoron that decays nonrelativistically is severely constrained. In particular, a lepton-number breaking scale above 300 GeV is excluded when the majoron mass is within [10⁻⁵, 1] MeV. The constraint is less strict with a smaller primordial abundance or equivalently, a higher freeze-out temperature. For $T_{\rm fo} > 100$ GeV, which corresponds to the smallest primordial abundance that can be induced from relativistic freeze-out, we find that a breaking scale f > 2 TeV is already excluded by the current Planck measurements for $m_J \in [10^{-5}, 1]$ MeV.

Note that for f < 1 GeV, the majoron decay generally occurs in the relativistic regime, as can be inferred from figure 3. Therefore, we concentrate on f > 1 GeV. Also, it is worthwhile to mention that for a lighter majoron around the eV scale, the nonrelativistic decay could occur after the epochs of matter-radiation equality and recombination when effects on, e.g., the structure formation and the neutrino free-streaming become significant [29]. On the other hand, for a heavier majoron above the MeV scale, the decay channel to electron-positron pairs opens. Besides, the majoron decay to neutrinos and electron-positron pairs could occur during the epochs of the BBN and neutrino decoupling and have observable effects. In particular, for $1 \text{ MeV} \lesssim m_J \lesssim 100 \text{ MeV}$, the most stringent constraint on f comes from Supernova 1987A. The absence of observing 100 MeV-range neutrino events from Supernova 1987A puts a lower

bound on the lepton-number breaking scale: $f \gtrsim 0.1 \,\text{GeV} \,(m_J/\text{MeV})$ [55]. See also [56, 57] for further discussions. It would be interesting to further investigate these nontrivial effects outside the mass region shown in figure 3, which goes beyond the scope of the current work.

5 The sandwiched window from precision $N_{\rm eff}$ measurements

We have seen from figure 3 that the current Planck measurements of $N_{\rm eff}$ can already put strict upper bounds on the lepton-number breaking scale for the scenario where the majoron decays nonrelativistically with a primordial abundance (FONR). On the other hand, in section 3.3 we demonstrated that the majoron abundance can also be accumulated through the freeze-in production $2\nu \to J$ and later decays nonrelativistically back to the neutrinos (FINR). As discussed in section 3.4, the FINR case can lead to a maximal $\Delta N_{\rm eff} \sim \mathcal{O}(0.1)$, which is beyond the sensitivity of the current Planck measurements.

However, the forecast sensitives of $\Delta N_{\rm eff}$ measurements in the future CMB experiments will be increased by a factor of a few. For instance, the SO experiment [22, 23] has a projected 2σ sensitivity $\Delta N_{\rm eff} < 0.1$, while the CMB-S4 experiment [24, 25] is expected to have a 2σ sensitivity $\Delta N_{\rm eff} < 0.06$. Therefore, for future CMB experiments, the FINR case can also be probed. Furthermore, due to the opposite dependence of $\Delta N_{\rm eff}$ on m_J and f between the FONR and the FINR cases, one can expect that the viable parameter space of the lepton-number breaking scale would be pushed into a narrow sandwiched window when the contributions from the FONR and FINR cases coexist. In particular, null signals of the $N_{\rm eff}$ excess in future CMB experiments could even close such a window and completely exclude the model.

To see the sandwiched window more clearly, we first consider the bounds from the FONR and FINR cases separately. That is, the bound from one case is derived without the contribution from the other case. In figure 4, we show the sandwiched window for the lepton-number breaking scale from the constraints of future SO and CMB-S4 experiments at 2σ level. Note that for the FONR case, the constraints depend on the primordial majoron abundances, which are characterized by $\Delta N_{\rm eff}^{\rm BBN}$, i.e., the contributions of the primordial relativistic majoron at the BBN epoch (see table 1). For the FINR case, we apply the results derived in ref. [30] by replacing the effective majoron-neutrino coupling g_{ν} with the breaking scale via $f=0.05\,{\rm eV}/g_{\nu}$. It corresponds to mapping the model-independent results into the seesaw framework.

In the upper left panel of figure 4, we show the parameter space of m_J and f under the constraints of SO with a primordial majoron abundance characterized by $\Delta N_{\rm eff}^{\rm BBN} = 0.06$ (corresponding to $T_{\rm fo} = 397\,{\rm MeV}$). It can be seen that for such a primordial abundance, the excluded region from the FONR case happens to be adjacent to that from the FINR case, and there is no viable parameter space for nonrelativistic majoron decay. This implies that if an excess of $\Delta N_{\rm eff}^{\rm CMB} > 0.1$ is not observed by the future SO experiment at 2σ level, then the scenario with the freeze-out temperature $T_{\rm fo} < 397\,{\rm MeV}$ will be ruled out within the regime of nonrelativistic decay.

In the upper right panel of figure 4, the result is shown for a smaller primordial majoron abundance characterized by $\Delta N_{\rm eff}^{\rm BBN} = 0.027$ (corresponding to $T_{\rm fo} > 100 \, {\rm GeV}$). Since the primordial abundance is reduced, the excluded region from the FONR case is expected to be

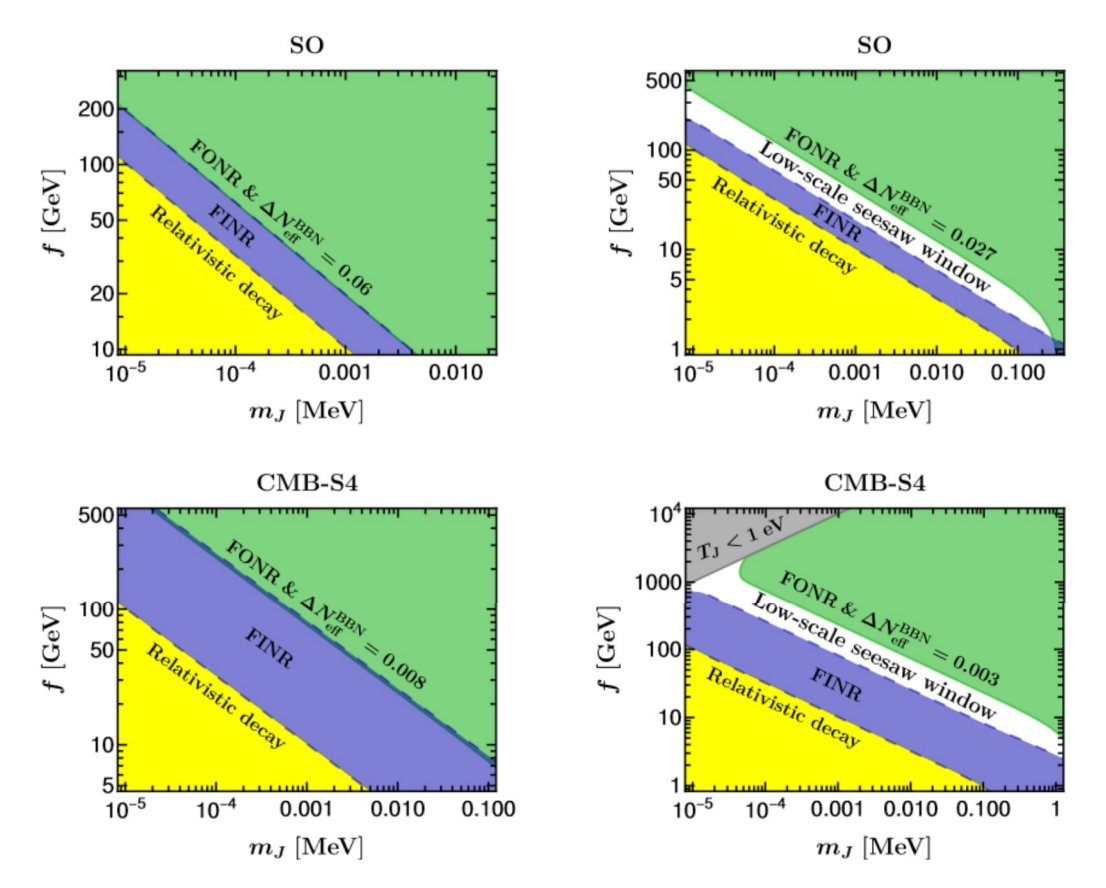


Figure 4. The sandwiched window for the lepton-number breaking scale from the constraints of the future SO (upper panel: $\Delta N_{\rm eff} < 0.1$) and CMB-S4 (lower panel: $\Delta N_{\rm eff} < 0.06$) experiments. In each subfigure, the green-shaded regions denote the excluded regions from the FONR case with different primordial majoron abundances (characterized by $\Delta N_{\rm eff}^{\rm BBN}$). The shaded regions in the lower left corner denote the regime of relativistic decay (yellow) and the regions excluded from the FINR cases (purple). The white bands labeled by "low-scale seesaw window" are the viable parameter space where the contributions from FONR and FINR cases coexist.

smaller than that in the upper left panel, thereby leaving a viable parameter space that is sandwiched by the constraints from the FONR and the FINR cases (denoted as "low-scale seesaw window"). For such a low-scale seesaw scenario, this is the parameter space where a minimal primordial majoron abundance inherited from relativistic freeze-out can survive, provided that no excess of $\Delta N_{\rm eff}^{\rm CMB} \geqslant 0.1$ is observed by the future SO experiment.

In the lower left and lower right panels of figure 4, the results are shown under the constraints of CMB-S4 with a primordial majoron abundance characterized by $\Delta N_{\rm eff}^{\rm BBN} = 0.008$ and $\Delta N_{\rm eff}^{\rm BBN} = 0.003$, respectively. We can infer from the lower left panel that the future CMB-S4 experiment is able to fully close the window for the low-scale seesaw scenario,

 $^{^9}$ Note that for $\Delta N_{\rm eff}^{\rm BBN} < 0.027$, the primordial majoron abundance cannot be inherited from the relativistic freeze-out (see figure 2). Smaller primordial abundances may be satisfied by other mechanisms (e.g., freeze-in production from the Higgs boson or RH neutrinos in the early Universe) or by the existence of extra relativistic degrees of freedom at high temperatures.

where the primordial majoron abundance comes from relativistic freeze-out and later decays nonrelativistically, provided that an excess of $\Delta N_{\rm eff}^{\rm CMB} \geqslant 0.06$ is not observed by CMB-S4 at 2σ level. Nevertheless, the case with a smaller primordial abundance ($\Delta N_{\rm eff}^{\rm BBN} < 0.008$) is still possible to survive if the abundance comes from other mechanism rather than relativistic freeze-out, as is shown in the lower right panel. This implies that even if the majoron itself as a relativistic species at the BBN epoch only contributes to $\Delta N_{\rm eff}$ at the order of 0.1%, its late-time nonrelativistic decay can generate observable effects in the future CMB experiments.

Finally, it should be noted that the above analysis is based on the assumptions that the bounds from the FONR and FINR cases are treated separately. For the real situation, the contribution to $\Delta N_{\rm eff}$ from neutrino coalescence $2\nu \to J$ should also be taken into account in the FONR case. In this case, one expects that the sandwiched window in figure 4 will become somewhat narrower. This can be understood by the fact that the contribution to $\Delta N_{\rm eff}$ at the CMB epoch for the real situation can always be divided into two parts

$$\Delta N_{\text{eff}}^{\text{CMB}} = \Delta N_{\text{eff}}^{\text{FO}} + \Delta N_{\text{eff}}^{\text{FI}}, \tag{5.1}$$

where $\Delta N_{\rm eff}^{\rm FO}$ ($\Delta N_{\rm eff}^{\rm FI}$) denotes the contribution from the primordial majoron abundance (neutrino coalescence). Since both $\Delta N_{\rm eff}^{\rm FO}$ and $\Delta N_{\rm eff}^{\rm FI}$ are non-negative, one will always obtain a larger $\Delta N_{\rm eff}$ than taking into account $\Delta N_{\rm eff}^{\rm FO}$ and $\Delta N_{\rm eff}^{\rm FI}$ separately. Therefore, the constraints and exclusion regions that we obtained in figure 4 should be considered as the most conservative results. Nevertheless, since $\Delta N_{\rm eff}^{\rm FI}$ can reach a maximal value at the order of 0.1 and the dependence of $\Delta N_{\rm eff}^{\rm FI}$ on m_J and f is opposite to $\Delta N_{\rm eff}^{\rm FO}$, it justifies our treatment as a good approximation to visualize the sandwiched window.

Before closing this section, we briefly comment on the applicability of our results to other well-motivated scenarios that feature lepton-number violations. In the low-scale type-I seesaw framework concerned here, the Dirac Yukawa coupling is highly suppressed by the active neutrino mass, i.e., $Y_{\nu} \sim \sqrt{m_i f}/v \lesssim 10^{-5}$. Such small couplings could be evaded, e.g., in the framework of the inverse seesaw model [58]. In the inverse seesaw scheme, apart from three RH neutrinos $N_{\rm R}$, one introduces another three singlets $N_{\rm L}$. The Lagrangian is given by

$$\mathcal{L} = -\overline{\ell_{L}}Y_{\nu}\widetilde{\Phi}N_{R} - \overline{N_{L}}MN_{R} - \frac{1}{2}\overline{N_{L}}Y_{N}'N_{L}^{c}S + \text{h.c.}, \qquad (5.2)$$

where M is the mass scale of heavy sterile neutrinos. The Majorana mass $\mu = Y_N' f/\sqrt{2}$ explicitly breaks lepton-number symmetry and thus can be very small in a technically natural way [59]. Assuming the hierarchy $\mu \ll Y_{\nu}v \ll M$, the active neutrino mass is given by: $m_{\nu} \sim Y_{\nu}^2 v^2 \mu/M^2$, where we have suppressed the flavor indices for simplicity. Therefore, one can have an $\mathcal{O}(1)$ Yukawa coupling Y_{ν} in the low-scale inverse seesaw scenario since the active neutrino mass is naturally suppressed by small μ . In this case, we find the coupling between majoron and active neutrinos turns out to be $g_{\nu} \sim \sqrt{Y_N' m_{\nu}/f}$. Furthermore, if the lepton-number breaking scale f is around the electroweak scale, then we have $g_{\nu} \sim m_{\nu}/f$, which is the same order as the case of the type-I seesaw model [see eq. (2.6)]. Therefore, our above calculation of $\Delta N_{\rm eff}$ from majoron decay is also applicable to the inverse seesaw scheme.

While the majoron cannot serve as dark matter in the low-scale type-I seesaw scenario, the dark matter candidate can be readily accommodated in the model-dependent setup. In particular, under the inverse seesaw framework, some of the sterile neutrinos could be at the keV-MeV scale and play the role of warm dark matter [60]. For such warm dark matter, its contribution to $\Delta N_{\rm eff}$ is negligible due to the Lyman- α forest constraints [61].

6 Conclusions

In this work, we have focused on the low-scale seesaw scenario associated with a singlet majoron from the spontaneous global $\mathrm{U}(1)_L$ breaking, and investigated the constraints on the lepton-number breaking scale f from the cosmological measurements of N_{eff} . This provides a complementary approach to the collider searches for lepton-number violation and TeV-scale Majorana neutrinos.

For the low-scale seesaw scenario, the breaking scale f is expected to be not far above the electroweak scale, so the majoron can decay within the cosmological time scale. The majoron interactions in the early Universe have two possible effects on $N_{\rm eff}$ at the epoch of CMB. The first is that the majoron abundance is accumulated through freeze-in production $(2\nu \to J)$ after the electroweak gauge symmetry breaking, and later decays nonrelativistically back to neutrinos $(J \to 2\nu)$. This possibility has been widely discussed in the literature, where lower bounds of f were obtained. In this work, we mainly focused on the second possibility that was usually neglected in previous studies. That is, the majoron possesses a non-negligible primordial abundance, which is inherited from relativistic freeze-out and later depleted into neutrinos. This situation is quite common within the minimal framework, where the majoron gets thermalized in the SM bath through the interactions with RH neutrinos or the Higgs boson.

We have demonstrated that the primordial abundance has sizable modification to $\Delta N_{\rm eff}$ that can be probed by the current and future CMB experiments. If the majoron decays relativistically, the contribution to $\Delta N_{\rm eff}$ was shown in figure 2, which only depends on the freeze-out temperature. Things become more interesting if the majoron decays in the nonrelativistic regime. As was shown in figure 3, the current Planck measurements could already put severe constraints on the lepton-number breaking scale. More importantly, in this case, a larger f would lead to a larger $\Delta N_{\rm eff}$. Therefore, opposite to the freeze-in scenario, upper bounds of f are obtained from primordial majoron decay. Furthermore, when both the freeze-out and freeze-in abundances coexist, we obtain a sandwiched window for f in terms of the majoron mass.

Given the forecast sensitivities of future SO and CMB-S4 experiments, we showed the sandwiched windows in figure 4. It can be seen that null signals of $\Delta N_{\rm eff}$ in future CMB experiments will push the low-scale seesaw scenario into a narrow sandwiched parameter space. In particular, if the primordial majoron abundance is inherited from relativistic freeze-out and later decays nonrelativistically into neutrinos, null signals of $\Delta N_{\rm eff}$ from CMB-S4 is able to fully close such a low-scale seesaw window.

Finally, although we have mainly focused on the majoron abundance in this work, it is worthwhile to emphasize that any new light particle coupled to neutrinos or photons can also be expected to result in a sandwiched window in the parameter space, as long as the particle has abundances from both the UV sources and the freeze-in production and

only decays after the neutrino decoupling. Such a general phenomenon deserves careful investigation in the future.

Acknowledgments

We would like to thank Xun-Jie Xu for helpful discussions. S.-P. Li is supported in part by the National Natural Science Foundation of China under grant No. 12141501 and also by CAS Project for Young Scientists in Basic Research (YSBR-099). BY is supported in part by the Natural Science Foundation of China under grant No. 11835013.

A Majoron interactions

In this appendix, we summarize the majoron interactions in the singlet majoron model. Most of the results in this section are not new and have been given in the literature but without details [31, 62]. Nevertheless, we would like to derive them here for the purpose of completeness and self-consistency, and also to set up our notations.

A.1 Majoron-neutrino interactions

First of all, before the electroweak gauge symmetry breaking, the majoron only couples to RH neutrinos. In this case, one can take the basis where the mass matrix of RH neutrinos is diagonal, i.e., $Y_N = \hat{Y}_N \equiv \text{Diag}(Y_1, Y_2, Y_3)$. Defining the mass eigenstates $\hat{N} \equiv N_R + N_R^c = (N_1, N_2, N_3)^T$, we can write $N_R = P_R \hat{N}$ and $N_R^c = P_L \hat{N}$ with $P_{R/L} \equiv (1 \pm \gamma_5)/2$ being the projection operators. Then we have

$$\overline{N_{\rm R}^c} N_{\rm R} = \overline{\hat{N}} P_{\rm R} \hat{N} , \qquad \overline{N_{\rm R}} N_{\rm R}^c = \overline{\hat{N}} P_{\rm L} \hat{N} . \tag{A.1}$$

Therefore, from eq. (2.1), we arrive at the interaction between the majoron and RH neutrinos:

$$\mathcal{L}_{J} = -\frac{\mathrm{i}J}{2\sqrt{2}}\overline{N_{\mathrm{R}}^{c}}\widehat{Y}_{N}N_{\mathrm{R}} + \frac{\mathrm{i}J}{2\sqrt{2}}\overline{N_{\mathrm{R}}}\widehat{Y}_{N}N_{\mathrm{R}}^{c} = -\frac{\mathrm{i}J}{2\sqrt{2}}\sum_{i=1}^{3}Y_{i}\overline{N_{i}}\gamma_{5}N_{i}. \tag{A.2}$$

After the electroweak gauge symmetry breaking, the Higgs boson acquires the non-zero VEV and the majoron will interact with active neutrinos through the flavor mixing between active and sterile neutrinos. The relevant Lagrangian reads

$$\mathcal{L} = -\overline{\nu_{L}} M_{D} N_{R} - \frac{1}{2} \overline{N_{R}^{c}} M_{R} N_{R} - \frac{iJ}{2\sqrt{2}} \overline{N_{R}^{c}} Y_{N} N_{R} + \text{h.c.}$$

$$= -\frac{1}{2} \left(\overline{\nu_{L}} \ \overline{N_{R}^{c}} \right) \begin{pmatrix} 0 & M_{D} \\ M_{D}^{T} & M_{R} \end{pmatrix} \begin{pmatrix} \nu_{L}^{c} \\ N_{R} \end{pmatrix} - \frac{iJ}{2\sqrt{2}} \overline{N_{R}^{c}} Y_{N} N_{R} + \text{h.c.}, \tag{A.3}$$

where $M_{\rm D}=Y_{\nu}v/\sqrt{2}$ is the Dirac mass matrix. The 6 × 6 mass matrix in eq. (A.3) can be diagonalized via

$$\mathcal{U}^{\dagger} \begin{pmatrix} 0 & M_{\rm D} \\ M_{\rm D}^{\rm T} & M_{\rm R} \end{pmatrix} \mathcal{U}^* = \begin{pmatrix} \widehat{m} & 0 \\ 0 & \widehat{M} \end{pmatrix}, \qquad \mathcal{U} \equiv \begin{pmatrix} V & R \\ S & U \end{pmatrix}, \tag{A.4}$$

where $\widehat{m} = \text{Diag}(m_1, m_2, m_3)$ and $\widehat{M} = \text{Diag}(M_1, M_2, M_3)$ are the diagonal mass matrices for light and heavy neutrinos, respectively. Here we have explicitly split the 6×6 unitary matrix \mathcal{U} into four 3×3 sub-matrices V, R, S and U. From eq. (A.4) and the unitarity of \mathcal{U} , one can obtain the following conditions

$$V^{\dagger}V + S^{\dagger}S = U^{\dagger}U + R^{\dagger}R = 1, \qquad (A.5)$$

$$V^{\dagger}R + S^{\dagger}U = \mathbf{0}, \tag{A.6}$$

$$V\widehat{m}V^{\mathrm{T}} + R\widehat{M}R^{\mathrm{T}} = \mathbf{0}, \tag{A.7}$$

which will be useful later. Changing from the flavor eigenstates to the mass eigenstates via

$$\nu_{\rm L} = V \widehat{\nu}_{\rm L} + R \widehat{N}_{\rm R}^c,
N_{\rm R} = S^* \widehat{\nu}_{\rm L}^c + U^* \widehat{N}_{\rm R},$$
(A.8)

the mass term in eq. (A.3) becomes

$$\mathcal{L}_{\text{mass}} = -\frac{1}{2} \left(\overline{\widehat{\nu}_{L}} \ \overline{\widehat{N}_{R}^{c}} \right) \begin{pmatrix} \widehat{m} & 0 \\ 0 & \widehat{M} \end{pmatrix} \begin{pmatrix} \widehat{\nu}_{L}^{c} \\ \widehat{N}_{R} \end{pmatrix} + \text{h.c.}$$

$$= -\frac{1}{2} \sum_{i=1}^{3} \left(m_{i} \overline{\nu}_{i} \nu_{i} + M_{i} \overline{N}_{i} N_{i} \right), \tag{A.9}$$

where we have defined $\hat{\nu}_L + \hat{\nu}_L^c \equiv \hat{\nu} = (\nu_1, \nu_2, \nu_3)^T$ and $\hat{N}_R + \hat{N}_R^c \equiv \hat{N} = (N_1, N_2, N_3)^T$. In the meanwhile, the interaction term in eq. (A.3) becomes

$$\mathcal{L}_{J} = -\frac{\mathrm{i}J}{2f} \left(\widehat{\nu}_{L} S^{\dagger} + \widehat{N}_{R}^{c} U^{\dagger} \right) \left(S \widehat{m} S^{\mathrm{T}} + U \widehat{M} U^{\mathrm{T}} \right) \left(S^{*} \widehat{\nu}_{L}^{c} + U^{*} \widehat{N}_{R} \right) + \mathrm{h.c.}$$

$$= -\frac{\mathrm{i}J}{2f} \left(\widehat{\nu}_{L} \ \widehat{N}_{R}^{c} \right) \begin{pmatrix} S^{\dagger}S \ S^{\dagger}U \\ U^{\dagger}S \ U^{\dagger}U \end{pmatrix} \begin{pmatrix} \widehat{m} \ 0 \\ 0 \ \widehat{M} \end{pmatrix} \begin{pmatrix} S^{\dagger}S \ S^{\dagger}U \\ U^{\dagger}S \ U^{\dagger}U \end{pmatrix}^{*} \begin{pmatrix} \widehat{\nu}_{L}^{c} \\ \widehat{N}_{R} \end{pmatrix} + \mathrm{h.c.}$$

$$= -\frac{\mathrm{i}J}{2f} \left(\widehat{\nu}_{L} \ \widehat{N}_{R}^{c} \right) \left[\begin{pmatrix} \mathbf{1} \ \mathbf{0} \\ \mathbf{0} \ \mathbf{1} \end{pmatrix} - \begin{pmatrix} V^{\dagger}V \ V^{\dagger}R \\ R^{\dagger}V \ R^{\dagger}R \end{pmatrix} \right] \begin{pmatrix} \widehat{m} \ 0 \\ 0 \ \widehat{M} \end{pmatrix}$$

$$\times \left[\begin{pmatrix} \mathbf{1} \ \mathbf{0} \\ \mathbf{0} \ \mathbf{1} \end{pmatrix} - \begin{pmatrix} V^{\dagger}V \ V^{\dagger}R \\ R^{\dagger}V \ R^{\dagger}R \end{pmatrix}^{*} \right] \begin{pmatrix} \widehat{\nu}_{L}^{c} \\ \widehat{N}_{R} \end{pmatrix} + \mathrm{h.c.}, \tag{A.10}$$

where in the third line we have used the unitarity conditions in eqs. (A.5) and (A.6). To simplify the notation, it is helpful to define $n_{\rm L} \equiv \left(\widehat{\nu}_{\rm L}, \widehat{N}_{\rm R}^c\right)^{\rm T}$ and $n_{\rm L} + n_{\rm L}^c \equiv n = (n_1, n_2, \dots, n_6)^{\rm T}$, where n_i (for i=1,2,3) correspond to the mass eigenstates of active neutrinos while n_i (for i=4,5,6) correspond to those of sterile neutrinos. Then it follows that $\overline{n_{\rm L}}n_{\rm L}^c = \overline{n}P_{\rm R}n$ and $\overline{n_{\rm L}^c}n_{\rm L} = \overline{n}P_{\rm L}n$. In addition, we define

$$C \equiv \begin{pmatrix} V^{\dagger} V & V^{\dagger} R \\ R^{\dagger} V & R^{\dagger} R \end{pmatrix}, \qquad \widehat{\mathcal{M}} \equiv \begin{pmatrix} \widehat{m} & 0 \\ 0 & \widehat{M} \end{pmatrix} \equiv \operatorname{Diag}(m_1, m_2, \dots, m_6). \tag{A.11}$$

Note that the (i,j) element of $\mathcal C$ can be related to the elements of the unitary matrix $\mathcal U$ via

$$C_{ij} = \sum_{k=1}^{3} U_{ki}^* U_{kj}, \qquad i, j = 1, 2, \dots, 6.$$
(A.12)

With above notations, eq. (A.10) can be reduced to

$$\mathcal{L}_{J} = -\frac{\mathrm{i}J}{2f}\overline{n_{\mathrm{L}}}\left[\widehat{\mathcal{M}} - \left(\widehat{\mathcal{C}}\widehat{\mathcal{M}} + \widehat{\mathcal{M}}\widehat{\mathcal{C}}^{*}\right) + \widehat{\mathcal{C}}\widehat{\mathcal{M}}\widehat{\mathcal{C}}^{*}\right]n_{\mathrm{L}}^{c} + \mathrm{h.c.}$$
(A.13)

Using eq. (A.7), it is straightforward to obtain $\widehat{\mathcal{CMC}}^* = \mathbf{0}$. Therefore, we are left with

$$\mathcal{L}_{J} = -\frac{\mathrm{i}J}{2f} \left[\left(\overline{n_{\mathrm{L}}} \widehat{\mathcal{M}} n_{\mathrm{L}}^{c} - \overline{n_{\mathrm{L}}^{c}} \widehat{\mathcal{M}} n_{\mathrm{L}} \right) - \left(\overline{n_{\mathrm{L}}} \left(\mathcal{C} \widehat{\mathcal{M}} + \widehat{\mathcal{M}} \mathcal{C}^{*} \right) n_{\mathrm{L}}^{c} - \overline{n_{\mathrm{L}}^{c}} \left(\mathcal{C}^{*} \widehat{\mathcal{M}} + \widehat{\mathcal{M}} \mathcal{C} \right) n_{\mathrm{L}} \right) \right]
= -\frac{\mathrm{i}J}{2f} \sum_{i,j=1}^{6} \left[m_{i} \overline{n_{i}} \gamma_{5} n_{i} - \left(\mathcal{C} \widehat{\mathcal{M}} + \widehat{\mathcal{M}} \mathcal{C}^{*} \right)_{ij} \overline{n_{i}} P_{\mathrm{R}} n_{j} + \left(\mathcal{C}^{*} \widehat{\mathcal{M}} + \widehat{\mathcal{M}} \mathcal{C} \right)_{ij} \overline{n_{i}} P_{\mathrm{L}} n_{j} \right]
= -\frac{\mathrm{i}J}{2f} \sum_{i,j=1}^{6} \left[m_{i} \overline{n_{i}} \gamma_{5} n_{i} - \left(m_{i} + m_{j} \right) \operatorname{Re} \mathcal{C}_{ij} \overline{n_{i}} \gamma_{5} n_{j} + \mathrm{i} \left(m_{i} - m_{j} \right) \operatorname{Im} \mathcal{C}_{ij} \overline{n_{i}} n_{j} \right]
= -\frac{\mathrm{i}J}{2f} \sum_{i,j=1}^{6} \overline{n_{i}} \left[\gamma_{5} \left(m_{i} + m_{j} \right) \left(\frac{1}{2} \delta_{ij} - \operatorname{Re} \mathcal{C}_{ij} \right) + \mathrm{i} \left(m_{i} - m_{j} \right) \operatorname{Im} \mathcal{C}_{ij} \right] n_{j}, \tag{A.14}$$

which is the general majoron-neutrino interaction given in eq. (2.4). Below we consider some special scenarios of the general interaction:

• For i, j = 1, 2, 3, from eq. (A.12) we have $C_{ij} = \delta_{ij} - \mathcal{O}\left(M_{\mathrm{D}}^2/M_{\mathrm{R}}^2\right) \simeq \delta_{ij}$, leading to

$$\mathcal{L}_{J\nu\nu} \simeq \frac{iJ}{2f} \sum_{i=1}^{3} m_i \overline{\nu_i} \gamma_5 \nu_i \,. \tag{A.15}$$

Therefore, the interaction between the majoron and the active neutrinos is approximately diagonal and is suppressed by m_i/f .

• For i, j = 4, 5, 6, we have $C_{ij} \sim \mathcal{O}\left(M_{\mathrm{D}}^2/M_{\mathrm{R}}^2\right)$, therefore

$$\mathcal{L}_{JNN} \simeq -\frac{\mathrm{i}J}{2f} \sum_{i=1}^{3} M_i \overline{N_i} \gamma_5 N_i \,, \tag{A.16}$$

which means the interaction between the majoron and the sterile neutrinos is also approximately diagonal.

• For i = 1, 2, 3 and j = 4, 5, 6, we have $C_{ij} \sim \mathcal{O}\left(M_{\rm D}/M_{\rm R}\right)$ and

$$\mathcal{L}_{J\nu N} \simeq \frac{iJ}{2f} \sum_{i=1}^{3} \sum_{j=4}^{6} m_j \overline{n_i} \left(\gamma_5 \operatorname{Re} \mathcal{C}_{ij} + i \operatorname{Im} \mathcal{C}_{ij} \right) n_j.$$
 (A.17)

This describes the interaction among the majoron, the active neutrinos and the sterile neutrinos.

The corresponding Feynman rules for majoron-neutrino interactions are summarized in figure 5.

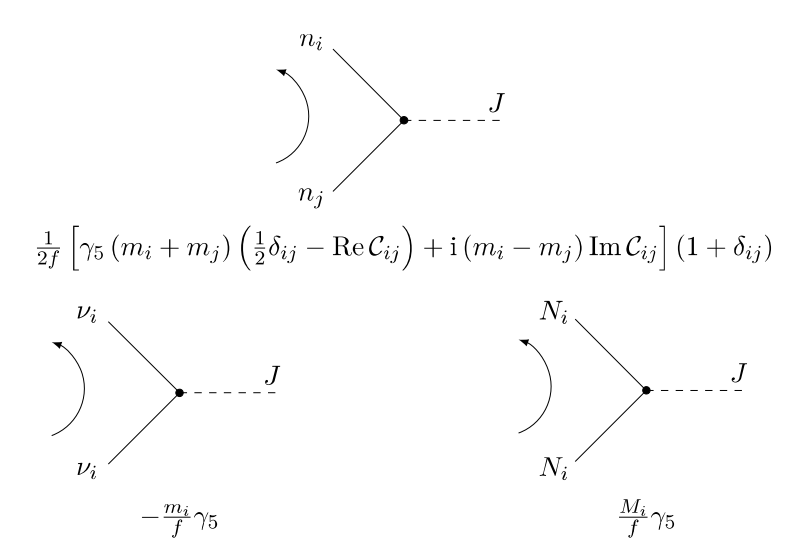


Figure 5. Feynman rules for the majoron-neutrino interactions. The arc arrows denote the orientations of fermion flow [63]. We have identified $\nu_i \equiv n_i$ and $N_i \equiv n_{i+3}$ (for i=1,2,3). Note that when i=j, there is a factor of 2! due to the two indistinguishable neutrinos. This is why there is an additional factor of $(1 + \delta_{ij})$ compared with eq. (A.14).

A.2 Majoron-Higgs interactions

When extended with a complex singlet S, the general scalar potential which obeys the gauge symmetry and global $U(1)_L$ symmetry is given by

$$V\left(\Phi,S\right) = \mu_{\Phi}^{2}\Phi^{\dagger}\Phi + \mu_{S}^{2}S^{\dagger}S + \frac{\lambda_{\Phi}}{2}\left(\Phi^{\dagger}\Phi\right)^{2} + \frac{\lambda_{S}}{2}\left(S^{\dagger}S\right)^{2} + \lambda_{\Phi S}\left(\Phi^{\dagger}\Phi\right)\left(S^{\dagger}S\right), \tag{A.18}$$

where

$$\Phi = \begin{pmatrix} G^{+} \\ \frac{v}{\sqrt{2}} + \frac{h' + iG^{0}}{\sqrt{2}} \end{pmatrix}, \qquad S = \frac{f}{\sqrt{2}} + \frac{\rho' + iJ}{\sqrt{2}}, \tag{A.19}$$

with Φ the SM Higgs doublet. Substituting the VEVs into the potential we have

$$V(v,f) \equiv V(\langle \Phi \rangle, \langle S \rangle) = \frac{1}{2} \mu_{\Phi}^2 v^2 + \frac{1}{2} \mu_S^2 f^2 + \frac{\lambda_{\Phi}^2}{8} v^4 + \frac{\lambda_S^2}{8} f^4 + \frac{\lambda_{\Phi S}}{4} v^2 f^2. \tag{A.20}$$

The VEVs are determined by minimizing the scalar potential,

$$\frac{1}{v}\frac{\partial}{\partial v}V\left(v,f\right) = \mu_{\Phi}^{2} + \frac{\lambda_{\Phi}}{2}v^{2} + \frac{\lambda_{\Phi S}}{2}f^{2} = 0, \tag{A.21}$$

$$\frac{1}{f}\frac{\partial}{\partial f}V\left(v,f\right) = \mu_{S}^{2} + \frac{\lambda_{S}}{2}f^{2} + \frac{\lambda_{\Phi S}}{2}v^{2} = 0, \tag{A.22}$$

from which we obtain

$$v = \sqrt{\frac{2(\lambda_{\Phi S}\mu_S^2 - \lambda_S\mu_{\Phi}^2)}{\lambda_{\Phi}\lambda_S - \lambda_{\Phi S}^2}},$$
(A.23)

$$f = \sqrt{\frac{2\left(\lambda_{\Phi S}\mu_{\Phi}^2 - \lambda_{\Phi}\mu_S^2\right)}{\lambda_{\Phi}\lambda_S - \lambda_{\Phi S}^2}}.$$
(A.24)

Note that in the limit of $\lambda_{\Phi S} \to 0$, the VEVs reduce to $v = \sqrt{-2\mu_{\Phi}^2/\lambda_{\Phi}}$ and $f = \sqrt{-2\mu_{S}^2/\lambda_{S}}$.

To calculate the spectrum of scalars in the singlet majoron model, we substitute eq. (A.19) into eq. (A.18) and keep only quadratic terms, obtaining

$$V \supset \frac{\lambda_{\Phi}}{2} v^2 h'^2 + \frac{\lambda_S}{2} f^2 \rho'^2 + \lambda_{\Phi S} v f h' \rho' = \frac{1}{2} \left(h' \ \rho' \right) \begin{pmatrix} \lambda_{\Phi} v^2 & \lambda_{\Phi S} v f \\ \lambda_{\Phi S} v f & \lambda_S f^2 \end{pmatrix} \begin{pmatrix} h' \\ \rho' \end{pmatrix}, \quad (A.25)$$

where eqs. (A.23) and (A.24) have been used to eliminate the quadratic terms of G^{\pm} , G^{0} and J. Therefore, we are left with four Nambu-Goldstone bosons

$$m_{G^{\pm}} = m_{G^0} = m_J = 0.$$
 (A.26)

Among them, G^{\pm} and G^0 will be absorbed into the longitudinal components of gauge bosons, while J will be left massless because it does not participate in any gauge interaction.

The mass of J can be generated, for example, by introducing terms that explicitly break the global $\mathrm{U}(1)_L$ symmetry [11, 18–21]. A simple way for generating the majoron mass is to add a tree-level $\mathrm{U}(1)_L$ -breaking term:

$$\lambda_b S^2 \Phi^{\dagger} \Phi$$
, (A.27)

such that the majoron gets a tree-level mass $m_J^2 = \lambda_b v^2/2$. For $m_J < 1\,\mathrm{MeV}$, we arrive at $\lambda_b < 10^{-11}$. It should be mentioned that such a small coupling cannot help to thermalize the majoron, as was pointed below eq. (2.12). In addition, while the majoron abundance can be generated by the freeze-in Higgs decay $h \to 2J$, it is much suppressed with respect to the neutrino coalescence $2\nu \to J$, as the former already eases at $T \simeq \mathcal{O}(m_h) \gg m_J$. Therefore, the impacts on the cosmological evolution of the majoron from this simple case can be safely neglected.

In addition, the mass eigenstates of the two CP-even neutral scalars $\{h, \rho\}$ are given by diagonalizing the mass matrix in eq. (A.25),

$$\begin{pmatrix} h \\ \rho \end{pmatrix} = \begin{pmatrix} \cos \theta & \sin \theta \\ -\sin \theta & \cos \theta \end{pmatrix} \begin{pmatrix} h' \\ \rho' \end{pmatrix}, \tag{A.28}$$

where the mixing angle results from the Higgs portal coupling $\lambda_{\Phi S}$, with

$$\tan 2\theta = \frac{2\lambda_{\Phi S} \tan \beta}{\lambda_{\Phi}^2 \tan^2 \beta - \lambda_S^2} \qquad \left(\tan \beta \equiv \frac{v}{f}\right). \tag{A.29}$$

Moreover, the masses turn out to be

$$m_h = \sqrt{\lambda_{\Phi} v^2 \cos^2 \theta + \lambda_S f^2 \sin^2 \theta + \lambda_{\Phi S} v f \sin 2\theta}, \qquad (A.30)$$

$$m_{\rho} = \sqrt{\lambda_S f^2 \cos^2 \theta + \lambda_{\Phi} v^2 \sin^2 \theta - \lambda_{\Phi S} v f \sin 2\theta}. \tag{A.31}$$

In the limit of $\lambda_{\Phi S} \to 0$ we have $m_h = \sqrt{\lambda_{\Phi}} v$ and $m_{\rho} = \sqrt{\lambda_S} f$.

The majoron self-interaction comes from the term proportional to λ_S , while the interaction between the majoron and the Higgs field comes from the term proportional to $\lambda_{\Phi S}$. More

explicitly, we have

$$\mathcal{L}_{J} = -\frac{\lambda_{S}}{8} \left(J^{4} + 2J^{2} \rho'^{2} + 4fJ^{2} \rho' \right) - \frac{\lambda_{\Phi S}}{4} \left(2J^{2}G^{-}G^{+} + J^{2} \left(G^{0} \right)^{2} + J^{2}h'^{2} + 2vJ^{2}h' \right) \\
= -\frac{\lambda_{S}}{8} J^{4} - \frac{\lambda_{\Phi S}}{2} J^{2}G^{-}G^{+} - \frac{\lambda_{\Phi S}}{4} J^{2} \left(G^{0} \right)^{2} \\
- \frac{1}{4} \left(\lambda_{S} \cos^{2}\theta + \lambda_{\Phi S} \sin^{2}\theta \right) J^{2}\rho^{2} - \frac{1}{2} \left(\lambda_{S}f \cos\theta - \lambda_{\Phi S}v \sin\theta \right) J^{2}\rho \\
- \frac{1}{4} \left(\lambda_{\Phi S} \cos^{2}\theta + \lambda_{S} \sin^{2}\theta \right) J^{2}h^{2} - \frac{1}{2} \left(\lambda_{\Phi S}v \cos\theta + \lambda_{S}f \sin\theta \right) J^{2}h \\
- \frac{1}{4} \left(\lambda_{S} - \lambda_{\Phi S} \right) \sin 2\theta J^{2}\rho h . \tag{A.32}$$

The Feynman rules for the majoron self-interaction and majoron-Higgs interactions are summarized in figure 6.

B Neutrino coalescence rate

The collision term of the neutrino coalescence $2\nu \to J$ in eq. (3.11) is given by

$$C_{2\nu\to J}^n = \int \frac{\mathrm{d}^3 p}{(2\pi)^3 2E} \frac{\mathrm{d}^3 p_1}{(2\pi)^3 2E_1} \frac{\mathrm{d}^3 p_2}{(2\pi)^2 2E_2} (2\pi)^4 \delta^4 |\mathcal{M}|_{2\nu\to J}^2 f_1(E_1) f_2(E_2) , \qquad (B.1)$$

where $\delta^4 \equiv \delta^4(p_1+p_2-p)$, and the quantum statistics for J is neglected. $f_i(E_i) = (e^{E_i/T_{\nu}}+1)^{-1}$ are distribution functions of incoming neutrinos, with T_{ν} the neutrino temperature, and the squared amplitude is given by

$$|\mathcal{M}|_{2\nu\to J}^2 \simeq \frac{2m_J^2}{f^2} \sum_{i=1}^3 m_i^2$$
 (B.2)

To calculate eq. (B.1), we can first go to the rest frame of J. Suppose in the rest plasma frame with 4-velovity $u^{\mu}=(1,\vec{0})$, the 4-momentum of the majoron is denoted by $p^{\mu}=(E,\vec{p})$. Then changing to the rest frame of J with $p'^{\mu}=(m_J,\vec{0})$ is equivalent to boosting the rest plasma frame with $u'^{\mu}=(E/m_J,-\vec{p}/m_J)$. In the rest frame of J, we denote the neutrino 4-momenta by $p'^{\mu}_{1,2}=(\omega_{1,2},\vec{q}_{1,2})$, where $\omega_1=\omega_2=m_J/2$, $|\vec{q}_1|=|\vec{q}_2|=\beta_{\nu}m_J/2$ are determined by the momentum conservation, with $\beta_{\nu}\equiv\sqrt{1-4m_i^2/m_J^2}$ the neutrino velocity. Then, in the rest frame of J, the collision term is given by

$$\mathcal{C}_{2\nu\to J}^{n} = \int \frac{\mathrm{d}^{3}p}{(2\pi)^{3}2E} \frac{\mathrm{d}^{3}q_{1}}{(2\pi)^{3}2\omega_{1}} \frac{\mathrm{d}^{3}q_{2}}{(2\pi)^{2}2\omega_{2}} (2\pi)^{4} \delta^{3}(\vec{q}_{1} + \vec{q}_{2}) \,\delta\left(2\sqrt{|\vec{q}_{1}|^{2} + m_{i}^{2}} - m_{J}\right) \\
\times |\mathcal{M}|_{2\nu\to J}^{2} f_{1}(p_{1}' \cdot u') f_{2}(p_{2}' \cdot u'), \tag{B.3}$$

where the distribution function of the thermalized neutrinos in the rest frame of J reads

$$f_i(p_i' \cdot u') = \frac{1}{e^{p_i' \cdot u'/T} + 1} = \frac{1}{e^{(E/2 + \vec{q}_i \cdot \vec{p}/m_J)/T_\nu} + 1},$$
 (B.4)

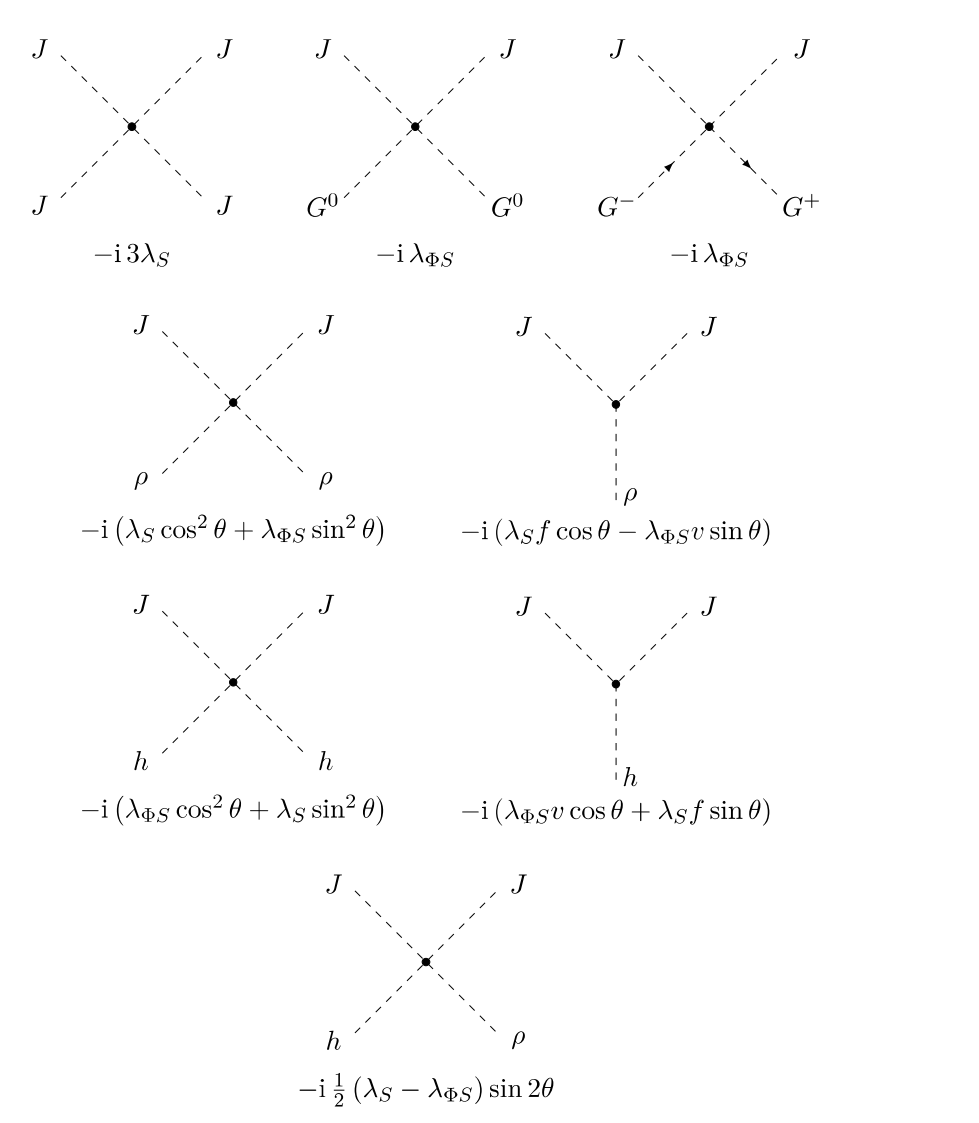


Figure 6. Feynman rules for the majoron self interaction and majoron-Higgs interactions, where θ is the mixing angle between two CP-even scalars ρ and h.

for i = 1, 2. Integrating out $|\vec{q}_2|$ and $|\vec{q}_1|$ via δ -functions, we are led to

$$C_{2\nu\to J}^{n} = \frac{\beta_{\nu}}{64\pi^{3}} |\mathcal{M}|_{2\nu\to J}^{2} \int_{0}^{\infty} \frac{p^{2} dp}{E} \int_{-1}^{1} d\cos\theta f_{1}(p'_{1} \cdot u') f_{2}(p'_{2} \cdot u')$$

$$= \frac{T_{\nu}}{16\pi^{3}} |\mathcal{M}|_{2\nu\to J}^{2} \int_{0}^{\infty} dp \frac{p}{E} \frac{1}{e^{E/T_{\nu}} + 1} \log\left(\frac{e^{\frac{E+\beta_{\nu}p}{2T_{\nu}}} + 1}{e^{\frac{E}{2T_{\nu}}} + e^{\frac{\beta_{\nu}p}{2T_{\nu}}}}\right), \tag{B.5}$$

Taking the Boltzmann approximation, we have

$$C_{2\nu\to J}^n \simeq \frac{\beta_{\nu}}{32\pi^3} |\mathcal{M}|_{2\nu\to J}^2 \int_0^\infty dE \sqrt{E^2 - m_J^2} \, e^{-E/T_{\nu}} \simeq \frac{T_{\nu} m_J^3}{16\pi^3 f^2} \sum_{i=1}^3 m_i^2 K_1(m_J/T_{\nu}) \,, \quad (B.6)$$

where in the last step we have assumed $m_i \ll m_J$ so that $\beta_{\nu} \simeq 1$, and K_1 is the modified Bessel function.

References

- [1] Planck collaboration, Planck 2018 results. Part VI. Cosmological parameters, Astron. Astrophys. 641 (2020) A6 [Erratum ibid. 652 (2021) C4] [arXiv:1807.06209] [INSPIRE].
- [2] T.-H. Yeh, J. Shelton, K.A. Olive and B.D. Fields, Probing physics beyond the standard model: limits from BBN and the CMB independently and combined, JCAP 10 (2022) 046 [arXiv:2207.13133] [INSPIRE].
- [3] Y. Chikashige, R.N. Mohapatra and R.D. Peccei, Are There Real Goldstone Bosons Associated with Broken Lepton Number?, Phys. Lett. B 98 (1981) 265 [INSPIRE].
- [4] P. Minkowski, $\mu \to e\gamma$ at a Rate of One Out of 10^9 Muon Decays?, Phys. Lett. B **67** (1977) 421 [INSPIRE].
- [5] T. Yanagida, Horizontal gauge symmetry and masses of neutrinos, Conf. Proc. C 7902131 (1979) 95 [INSPIRE].
- [6] M. Gell-Mann, P. Ramond and R. Slansky, Complex Spinors and Unified Theories, Conf. Proc. C 790927 (1979) 315 [arXiv:1306.4669] [INSPIRE].
- [7] S.L. Glashow, The Future of Elementary Particle Physics, in NATO Science Series B 61, Springer (1980), pp. 687–713 [DOI:10.1007/978-1-4684-7197-7_15] [INSPIRE].
- [8] R.N. Mohapatra and G. Senjanovic, Neutrino Mass and Spontaneous Parity Nonconservation, Phys. Rev. Lett. 44 (1980) 912 [INSPIRE].
- [9] V. Berezinsky and J.W.F. Valle, The KeV majoron as a dark matter particle, Phys. Lett. B 318 (1993) 360 [hep-ph/9309214] [INSPIRE].
- [10] M. Lattanzi and J.W.F. Valle, Decaying warm dark matter and neutrino masses, Phys. Rev. Lett. 99 (2007) 121301 [arXiv:0705.2406] [INSPIRE].
- [11] M. Frigerio, T. Hambye and E. Masso, Sub-GeV dark matter as pseudo-Goldstone from the seesaw scale, Phys. Rev. X 1 (2011) 021026 [arXiv:1107.4564] [INSPIRE].
- [12] F. Bazzocchi, M. Lattanzi, S. Riemer-Sørensen and J.W.F. Valle, X-ray photons from late-decaying majoron dark matter, JCAP 08 (2008) 013 [arXiv:0805.2372] [INSPIRE].
- [13] M. Lattanzi, S. Riemer-Sorensen, M. Tortola and J.W.F. Valle, Updated CMB and x- and γ-ray constraints on Majoron dark matter, Phys. Rev. D 88 (2013) 063528 [arXiv:1303.4685] [INSPIRE].
- [14] F.S. Queiroz and K. Sinha, The Poker Face of the Majoron Dark Matter Model: LUX to keV Line, Phys. Lett. B 735 (2014) 69 [arXiv:1404.1400] [INSPIRE].
- [15] C. Garcia-Cely and J. Heeck, Neutrino Lines from Majoron Dark Matter, JHEP 05 (2017) 102 [arXiv:1701.07209] [INSPIRE].
- [16] K. Akita and M. Niibo, Updated constraints and future prospects on majoron dark matter, JHEP 07 (2023) 132 [arXiv:2304.04430] [INSPIRE].
- [17] X.-J. Xu, S. Zhou and J. Zhu, The ν_R -philic scalar dark matter, arXiv:2310.16346 [INSPIRE].
- [18] P. Langacker, R.D. Peccei and T. Yanagida, Invisible Axions and Light Neutrinos: Are They Connected?, Mod. Phys. Lett. A 1 (1986) 541 [INSPIRE].
- [19] E.K. Akhmedov, Z.G. Berezhiani, R.N. Mohapatra and G. Senjanovic, *Planck scale effects on the majoron*, *Phys. Lett. B* **299** (1993) 90 [hep-ph/9209285] [INSPIRE].

- [20] I.Z. Rothstein, K.S. Babu and D. Seckel, Planck scale symmetry breaking and majoron physics, Nucl. Phys. B 403 (1993) 725 [hep-ph/9301213] [INSPIRE].
- [21] P.-H. Gu, E. Ma and U. Sarkar, *Pseudo-Majoron as Dark Matter*, *Phys. Lett. B* **690** (2010) 145 [arXiv:1004.1919] [INSPIRE].
- [22] SIMONS OBSERVATORY collaboration, The Simons Observatory: Science goals and forecasts, JCAP 02 (2019) 056 [arXiv:1808.07445] [INSPIRE].
- [23] SIMONS OBSERVATORY collaboration, The Simons Observatory: Astro2020 Decadal Project Whitepaper, Bull. Am. Astron. Soc. 51 (2019) 147 [arXiv:1907.08284] [INSPIRE].
- [24] CMB-S4 collaboration, CMB-S4 Science Book, First Edition, arXiv:1610.02743 [INSPIRE].
- [25] K. Abazajian et al., CMB-S4 Science Case, Reference Design, and Project Plan, arXiv:1907.04473 [INSPIRE].
- [26] Z. Chacko, L.J. Hall, T. Okui and S.J. Oliver, *CMB signals of neutrino mass generation*, *Phys. Rev. D* **70** (2004) 085008 [hep-ph/0312267] [INSPIRE].
- [27] C. Boehm, M.J. Dolan and C. McCabe, Increasing Neff with particles in thermal equilibrium with neutrinos, JCAP 12 (2012) 027 [arXiv:1207.0497] [INSPIRE].
- [28] M. Escudero and S.J. Witte, A CMB search for the neutrino mass mechanism and its relation to the Hubble tension, Eur. Phys. J. C 80 (2020) 294 [arXiv:1909.04044] [INSPIRE].
- [29] S. Sandner, M. Escudero and S.J. Witte, Precision CMB constraints on eV-scale bosons coupled to neutrinos, Eur. Phys. J. C 83 (2023) 709 [arXiv:2305.01692] [INSPIRE].
- [30] S.-P. Li and X.-J. Xu, N_{eff} constraints on light mediators coupled to neutrinos: the dilution-resistant effect, JHEP 10 (2023) 012 [arXiv:2307.13967] [INSPIRE].
- [31] A. Pilaftsis, Astrophysical and terrestrial constraints on singlet Majoron models, Phys. Rev. D 49 (1994) 2398 [hep-ph/9308258] [INSPIRE].
- [32] A.D. Dolgov and F.L. Villante, BBN bounds on active sterile neutrino mixing, Nucl. Phys. B 679 (2004) 261 [hep-ph/0308083] [INSPIRE].
- [33] S.-P. Li and X.-J. Xu, Dark matter produced from right-handed neutrinos, JCAP 06 (2023) 047 [arXiv:2212.09109] [INSPIRE].
- [34] S. Kanemura and S.-P. Li, Dark phase transition from WIMP: complementary tests from gravitational waves and colliders, JCAP 03 (2024) 005 [arXiv:2308.16390] [INSPIRE].
- [35] J. McDonald, Thermally generated gauge singlet scalars as selfinteracting dark matter, Phys. Rev. Lett. 88 (2002) 091304 [hep-ph/0106249] [INSPIRE].
- [36] A. Kusenko, Sterile neutrinos, dark matter, and the pulsar velocities in models with a Higgs singlet, Phys. Rev. Lett. 97 (2006) 241301 [hep-ph/0609081] [INSPIRE].
- [37] K. Petraki and A. Kusenko, Dark-matter sterile neutrinos in models with a gauge singlet in the Higgs sector, Phys. Rev. D 77 (2008) 065014 [arXiv:0711.4646] [INSPIRE].
- [38] L.J. Hall, K. Jedamzik, J. March-Russell and S.M. West, Freeze-In Production of FIMP Dark Matter, JHEP 03 (2010) 080 [arXiv:0911.1120] [INSPIRE].
- [39] G. Mangano, G. Miele, S. Pastor and M. Peloso, A Precision calculation of the effective number of cosmological neutrinos, Phys. Lett. B 534 (2002) 8 [astro-ph/0111408] [INSPIRE].
- [40] G. Mangano, G. Miele, S. Pastor, T. Pinto, O. Pisanti and P.D. Serpico, Relic neutrino decoupling including flavor oscillations, Nucl. Phys. B 729 (2005) 221 [hep-ph/0506164] [INSPIRE].

- [41] P.F. de Salas and S. Pastor, Relic neutrino decoupling with flavour oscillations revisited, JCAP 07 (2016) 051 [arXiv:1606.06986] [INSPIRE].
- [42] M. Escudero Abenza, Precision early universe thermodynamics made simple: N_{eff} and neutrino decoupling in the Standard Model and beyond, JCAP 05 (2020) 048 [arXiv:2001.04466] [INSPIRE].
- [43] K. Akita and M. Yamaguchi, A precision calculation of relic neutrino decoupling, JCAP 08 (2020) 012 [arXiv:2005.07047] [INSPIRE].
- [44] J. Froustey, C. Pitrou and M.C. Volpe, Neutrino decoupling including flavour oscillations and primordial nucleosynthesis, JCAP 12 (2020) 015 [arXiv:2008.01074] [INSPIRE].
- [45] J.J. Bennett et al., Towards a precision calculation of N_{eff} in the Standard Model. Part II. Neutrino decoupling in the presence of flavour oscillations and finite-temperature QED, JCAP 04 (2021) 073 [arXiv:2012.02726] [INSPIRE].
- [46] M. Cielo, M. Escudero, G. Mangano and O. Pisanti, N_{eff} in the Standard Model at NLO is 3.043, Phys. Rev. D 108 (2023) L121301 [arXiv:2306.05460] [INSPIRE].
- [47] G.-y. Huangs, T. Ohlsson and S. Zhou, Observational Constraints on Secret Neutrino Interactions from Big Bang Nucleosynthesis, Phys. Rev. D 97 (2018) 075009 [arXiv:1712.04792] [INSPIRE].
- [48] J. Venzor, A. Pérez-Lorenzana and J. De-Santiago, Bounds on neutrino-scalar nonstandard interactions from big bang nucleosynthesis, Phys. Rev. D 103 (2021) 043534 [arXiv:2009.08104] [INSPIRE].
- [49] S. Sarkar, Big bang nucleosynthesis and physics beyond the standard model, Rept. Prog. Phys. 59 (1996) 1493 [hep-ph/9602260] [INSPIRE].
- [50] R.H. Cyburt, B.D. Fields, K.A. Olive and T.-H. Yeh, Big Bang Nucleosynthesis: 2015, Rev. Mod. Phys. 88 (2016) 015004 [arXiv:1505.01076] [INSPIRE].
- [51] C. Pitrou, A. Coc, J.-P. Uzan and E. Vangioni, Precision big bang nucleosynthesis with improved Helium-4 predictions, Phys. Rep. **754** (2018) 1 [arXiv:1801.08023] [INSPIRE].
- [52] S. Borsanyi et al., Calculation of the axion mass based on high-temperature lattice quantum chromodynamics, Nature 539 (2016) 69 [arXiv:1606.07494] [INSPIRE].
- [53] I. Esteban, M.C. Gonzalez-Garcia, M. Maltoni, T. Schwetz and A. Zhou, The fate of hints: updated global analysis of three-flavor neutrino oscillations, JHEP 09 (2020) 178 [arXiv:2007.14792] [INSPIRE].
- [54] S. Gariazzo, P.F. de Salas and S. Pastor, Thermalisation of sterile neutrinos in the early Universe in the 3+1 scheme with full mixing matrix, JCAP 07 (2019) 014 [arXiv:1905.11290] [INSPIRE].
- [55] D.F.G. Fiorillo, G.G. Raffelt and E. Vitagliano, Strong Supernova 1987A Constraints on Bosons Decaying to Neutrinos, Phys. Rev. Lett. 131 (2023) 021001 [arXiv:2209.11773] [INSPIRE].
- [56] K. Akita, S.H. Im and M. Masud, Probing non-standard neutrino interactions with a light boson from next galactic and diffuse supernova neutrinos, JHEP 12 (2022) 050 [arXiv:2206.06852] [INSPIRE].
- [57] K. Akita, S.H. Im, M. Masud and S. Yun, Limits on heavy neutral leptons, Z' bosons and majorons from high-energy supernova neutrinos, arXiv:2312.13627 [INSPIRE].
- [58] R.N. Mohapatra and J.W.F. Valle, Neutrino Mass and Baryon Number Nonconservation in Superstring Models, Phys. Rev. D 34 (1986) 1642 [INSPIRE].

- [59] G. 't Hooft, Naturalness, chiral symmetry, and spontaneous chiral symmetry breaking, in NATO Science Series B 59, Springer (1980), pp. 135–157 [DOI:10.1007/978-1-4684-7571-5_9] [INSPIRE].
- [60] E. Fernandez-Martinez, M. Pierre, E. Pinsard and S. Rosauro-Alcaraz, *Inverse Seesaw, dark matter and the Hubble tension*, *Eur. Phys. J. C* 81 (2021) 954 [arXiv:2106.05298] [INSPIRE].
- [61] S.-P. Li, X.-Q. Li, X.-S. Yan and Y.-D. Yang, Simple estimate of BBN sensitivity to light freeze-in dark matter, Phys. Rev. D 104 (2021) 115007 [arXiv:2106.07122] [INSPIRE].
- [62] J. Schechter and J.W.F. Valle, Neutrino Decay and Spontaneous Violation of Lepton Number, Phys. Rev. D 25 (1982) 774 [INSPIRE].
- [63] A. Denner, H. Eck, O. Hahn and J. Kublbeck, Feynman rules for fermion number violating interactions, Nucl. Phys. B 387 (1992) 467 [INSPIRE].